Loss of Phosphoethanolamine *N*-Methyltransferases Abolishes Phosphatidylcholine Synthesis and Is Lethal[1][OPEN]

Weihua Chen,[a] Matthew C. Taylor,[b] Russell A. Barrow,[c] Mikaël Croyal,[d] and Josette Masle[a,2,3,4]

[a]Research School of Biology, The Australian National University, Canberra, Australian Capital Territory 2601, Australia
[b]Land and Water Flagship, Commonwealth Scientific and Industrial Research Organization, Canberra, Australian Capital Territory 2601, Australia
[c]Research School of Chemistry, The Australian National University, Canberra, Australian Capital Territory 2601, Australia
[d]CRNH Nantes, Mass Spectrometry Core facility, 8 Quai Moncousu BP–70721, Nantes cedex 1, France

ORCID IDs: 0000-0003-4192-1634 (W.C.); 0000-0001-9576-1555 (M.C.T.); 0000-0002-3248-1246 (R.A.B.); 0000-0003-3385-4937 (J.M.).

Plants use several pathways to synthesize phosphatidylcholine (PC), the major phospholipid of eukaryotic cells. PC has important structural and signaling roles. One pathway plants use for synthesis is the phospho-base methylation pathway, which forms the head-group phosphocholine through the triple methylation of phosphoethanolamine (PEA) catalyzed by phosphoethanolamine *N*-methyltransferases (PEAMTs). Our understanding of that pathway and its physiological importance remains limited. We recently reported that disruption of *Arabidopsis thaliana PEAMT1/NMT1* and *PEAMT3/NMT3* induces severe PC deficiency leading to dwarfism and impaired development. However, the double *nmt1 nmt3* knock-out mutant is viable. Here, we show that this is enabled by residual PEAMT activity through a third family member, NMT2. The triple *nmt1 nmt2 nmt3* knock-out mutant cannot synthesize PC from PEA and is lethal. This shows that, unlike mammals and yeast, Arabidopsis cannot form PC from phosphatidyl ethanolamine (PE), and demonstrates that methylation of PEA is the sole, and vital, entry point to PC synthesis. We further show that Arabidopsis has evolved an expanded family of four nonredundant PEAMTs through gene duplication and alternate use of the *NMT2* promoter. *NMT2* encodes two PEAMT variants, which greatly differ in their ability to perform the initial phospho-base methylation of PEA. Five amino acids at the N terminus of PEAMTs are shown to each be critical for the catalysis of that step committing to PC synthesis. As a whole, these findings open new avenues for enzymatic engineering and the exploration of ways to better tune phosphocholine and PC synthesis to environmental conditions for improved plant performance.

Phosphatidylcholine (PC) is a strong, bilayer-forming lipid and the major component of plasma membranes in most eukaryotes. Besides its structural role, PC is the source of signaling molecules, and it is also found bound to membrane proteins in mammals, participating directly in membrane-mediated signaling (Yeagle, 2016). It is also an important site for fatty acid desaturation in plants. In addition, its choline (Cho) head group can be oxidized to betaine, and in some plant species further metabolized to produce Gly betaine, a quaternary ammonium compound involved in osmo-regulation and other stress-protective mechanisms (Park et al., 2007; Chen and Murata, 2008).

The pathways for PC synthesis show some conservation among eukaryotes, but also fundamental differences. Yeast and mammals can synthesize PC via the cytidine-diphosphate (CDP)-choline pathway, also known as the Kennedy pathway (Supplemental Figure S1) (Kennedy and Weiss, 1956) where free Cho is phosphorylated to produce phosphocholine (PCho), subsequently converted to CDP-Cho. The Cho head-group is then transferred to diacylglycerol (DAG), forming PC. Another route is the phosphatidyl-base methylation pathway, or Bremer–Greenberg pathway, where PC is produced from phosphatidylethanolamine (PE) via three sequential methylations (Bremer and Greenberg, 1961; Kodaki and Yamashita, 1987; Summers et al., 1988;

[1]Funding: This research work was supported by The Australian National University and a Grains Research and Development Corporation grant (grant no. ANU00023 to J.M.).
[2]Author for contact: josette.masle@anu.edu.au.
[3]Present address: Research School of Biology, The Australian National University, Canberra ACT 2601, Australia.
[4]Senior author.
The author responsible for distribution of materials integral to the findings presented in this article in accordance with the policy described in the Instructions for Authors (www.plantphysiol.org) is: Josette Masle (josette.masle@anu.edu.au).
J.M. conceived and supervised the project; W.C. and J.M. designed the experiments; W.C., R.B., M.T., J.M. and M.C. performed the experiments; W.C. and J.M. analyzed the data; J.M. and W.C. wrote the manuscript.
[OPEN]Articles can be viewed without a subscription.
www.plantphysiol.org/cgi/doi/10.1104/pp.18.00694

McGraw and Henry, 1989; Cui et al., 1993; Preitschopf et al., 1993).

Plants have evolved an alternative, phospho-base methylation pathway catalyzed by phosphoethanolamine *N*-methyltransferases (PEAMTs), also present in *Plasmodium falciparum* and nematodes (Pessi et al., 2004; Brendza et al., 2007; Witola et al., 2008). Phosphoethanolamine (PEA) derived from Ser undergoes three successive methylations at the free phospho-base, forming PCho. PCho can then serve as the head group to form PC via the Kennedy pathway, or be dephosphorylated to produce Cho. Instead of being converted to PCho, the phosphomonomethylethanolamine (PMMEA) and phosphodimethylethanolamine (PDMEA) intermediates of that alternative methylation pathway can be diverted to the phosphatidyl-base methylation pathway to produce PtdMMEA and PtdDMEA, and finally PC through phospholipid *N*-methyltransferase (PLMT) enzymes (Keogh et al., 2009). The characterized PLMTs from both Arabidopsis (*Arabidopsis thaliana*) and soybean (*Glycine max*) are unable to use PE as a substrate (Keogh et al., 2009), and methylation activity of PEAMTs over PE has not been found in plant cells of various species, including in chase experiments with the Arabidopsis AtNMT1 using [^{32}P]PE (Bolognese and McGraw, 2000). No plant enzyme has so far been identified that can methylate PE to form PtMMEA, unlike in yeast and mammals (Hitz et al., 1981; Mudd and Datko, 1986; Datko and Mudd, 1988a, 1988b; Bolognese and McGraw, 2000; McNeil et al., 2000; Keogh et al., 2009). However, definite proof that none exist is still lacking. In their study of the amino-alcohol-phosphotransferase *aapt1* and *aapt2* mutants, Liu et al. (2015) recently proposed a hypothetical methylation pathway that might indirectly convert PE to PC in Arabidopsis, via the synthesis of lysophosphatidylethanolamine (LysoPE), followed by its methylation to lysophosphatidylcholine (LysoPC), and then conversion to PC by LysoPC acyltransferase or LysoPC transacylase. Furthermore, it remains to be genetically proven that plants do not possess enzymes capable of phosphatidyl-base methylation of PE to produce PtdMMEA and from there PtdDMEA and PC. In its current draft, the Arabidopsis genome does not appear to carry genes resembling the yeast or mammalian genes known to methylate PE. However, sequence homology can be a poor predictor of functional homology. Thus, the Arabidopsis and soybean PLMTs have only 25% identity with their yeast or rat functional homologs (Keogh et al., 2009). We reasoned that if the conversion of PEA to PMMEA is the unique entry point to PC synthesis, a total *peamt* knock-out mutant should be unable to synthesize PC.

The Arabidopsis genome encodes three PEAMT enzymes (Bolognese and McGraw, 2000; Lee and Jez, 2017; Chen et al., 2018). PEAMT1/NMT1 has been extensively studied and is the best-known plant PEAMT. When it is rendered nonfunctional through gene knockout, roots show developmental defects in tissue culture, and also cell death (Cruz-Ramírez et al., 2004). It is a phenotype also associated with PC deficiency in mammals. However, the aerial plant parts appear unaffected, and soil-grown plants develop normally (Cruz-Ramírez et al., 2004; Chen et al., 2018), although some male sterility has been reported in *NMT1* silencing lines under nonoptimal temperature conditions (Mou et al., 2002). Under optimal conditions, *nmt3* and *nmt2* single mutants appear normal (BeGora et al., 2010; Lee and Jez, 2017; Chen et al., 2018). However, we recently showed that when introduced into the *nmt1* background, the *nmt3* mutation causes general growth inhibition, dramatic developmental defects, and yield loss (Chen et al., 2018). All effects could be alleviated by an exogenous supply of Cho or PCho, consistent with the shared biochemical function of NMT3 and NMT1 as PEAMTs catalyzing the conversion of PEA to PCho. These results demonstrated that the phospho-base methylation pathway is a major contributor to PC synthesis in Arabidopsis, and that NMT1 and NMT3 have a dominant, critical role in regulating the flux of metabolites through that pathway and sustaining normal plant development.

However, left unresolved were the origin of the residual PC synthesis measured in the *nmt1 nmt3* mutant, and the roles of *NMT2*. There is scant and conflicting information on the biochemical function of NMT2. An early in vitro study reported that it could catalyze the methylation of PMMEA and PDMEA, but not the initial methylation of PEA (BeGora et al., 2010), while a very recent biochemical analysis of the in vitro kinetic parameters of Arabidopsis NMTs, including NMT2, concludes that NMT2 also catalyzes that first methylation (Lee and Jez, 2017). Moreover, nothing is known of NMT2 function and physiological roles in planta.

We had three aims in the current study. First, we wished to investigate the function of the *NMT2* gene. Second, we hoped to grasp its contribution to plant development and to residual PC synthesis in the *nmt1 nmt3* mutant. Third, we wanted to find out whether PEAMT activity and the *P*-base methylation pathway are absolutely required for PC synthesis in plants—Are they necessary to plant survival? For example, in mammals and *Caenorhabditis elegans,* disruption of PEAMT activity causes cell death unless Cho is exogenously provided (Palavalli et al., 2006; Brendza et al., 2007). In a study on *Plasmodium*, loss of PMT caused extreme growth and developmental defects but was not lethal in the absence of Cho supplementation; this result was ascribed to some residual Cho in the human erythrocytes (Witola et al., 2008). In plants this is unknown, as no total *peamt* knock-out mutant has yet been reported.

In this article we demonstrate that Arabidopsis NMT2 encodes two protein isoforms that both have the intrinsic capacity to catalyze the three sequential methylations of PEA to form PCho, but greatly differ in their catalytic efficiencies during the first methylation, and in their in planta contribution to PC synthesis. We rescue a triple *nmt1 nmt2 nmt3* knock-out mutant where transcription of the three genes is abolished, and we

demonstrate that this action abrogates PC synthesis and is lethal. These findings establish that PEA methylation catalyzed by PEAMT is the obligatory entry point for de novo PC synthesis in plants, which rules out the direct or indirect production of PC from PE. Results show that PC synthesis is absolutely necessary to plant life. In addition, we identify key residues at the N-terminal of PEAMTs that are essential to the catalysis of that first step under physiological conditions.

RESULTS

NMT2 Encodes Two PEAMT Isoforms through Alternative Use of Its Promoter

To assess the function of *NMT2*, we initially tested its ability to compensate for the loss of *NMT1* when driven by the *NMT1* promoter and allow normal root development. The full *NMT2* genomic sequence fused to the *NMT1* promoter was transformed into the previously characterized *nmt1* knock-out mutant, which shows a distinctive short root phenotype (Cruz- Ramírez et al., 2004; Chen et al., 2018). The transgene restored the wild-type root length (Fig. 1, A and B), indicating functional homology between NMT2 and NMT1 as PEAMT enzymes catalyzing the conversion of PEA to PCho. Supporting this, root and shoot growth in the *nmt1 nmt3* mutant responded to exogenous PEA supply (Fig. 1, C and D). Taken together, these results showed that PC synthesis in the *nmt1 nmt3* mutant originated, at least in part, from residual PEAMT activity, likely through NMT2 activity.

This result was at odds with the long-standing annotation of NMT2 as an enzyme only able to catalyze the second and third reaction of the phospho-base methylation pathway—but not the first (BeGora et al., 2010). This result led us to re-examine *NMT2* function and notice that the *NMT2* locus gives rise to two transcripts. These two transcripts, hereafter referred to as *NMT2.1* and *NMT2.2,* are initiated from different transcription start sites (TSS) (Fig. 2), indicating that they are generated through alternate use of the promoter. The gene structure and nucleotide sequence differences between them lie at the 5′ end. The 5′ untranslated region (UTR) of *NMT2.1* is part of the *NMT2.2* second exon and first intron. In addition to being longer, the 5′UTR of *NMT2.2* contains a conserved upstream open reading frame (uORF) that belongs to the Arabidopsis conserved uORF homology Group 13 (Hayden and Jorgensen, 2007), similar to the uORF present in *NMT3* and also in *NMT1,* where it has been shown to have important transcriptional and posttranscriptional regulatory roles (Tabuchi et al., 2006; Alatorre-Cobos et al., 2012). No such uORF is present in *NMT2.1.* The NMT2.1- and NMT2.2-deduced amino acid sequences are identical except for 16 additional amino acids at the N-terminal of NMT2.2 (Fig. 2B).

Functional Specificity between the NMT2.1 and NMT2.2 Isoforms

To compare the biochemical functions of the two NMT2 proteins, we expressed *NMT2.1* and *NMT2.2* cDNAs in the yeast *Saccharomyces cerevisiae* and used ^{31}P-NMR (NMR) to monitor PEAMT activity in crude cell protein extracts upon supplementation of PEA and *S*-adenosyl Met substrates (Fig. 1, E–H). The NMR spectra at the start of the reaction all showed a single peak, with a chemical shift of 3.79 ppm from the internal standard, matching that of the PEA standard (Fig. 1, E and F). For cells expressing the empty vector, no change was observed in the position and size of that peak, throughout the 94-h time course of the assays, and no PCho peak could be detected, at any time (Fig. 1H). In contrast, spectra obtained for protein extracts from cells expressing NMT2.2 showed the formation of a second peak, matching the position of the PCho standard (chemical shift of 3.27 ppm), and of increasing size as the reaction progressed, while the PEA peak concomitantly became smaller (Fig. 1E). Contrary to expectations (BeGora et al., 2010), cells expressing NMT2.1 showed a similar pattern. However, the PCho peak appeared with a delay and was smaller (Fig. 1F). The conversion rates of PEA to PCho after 4 d was only 14% as opposed to 34% for extracts from NMT2.2-expressing cells (Fig. 1G). These data indicated that the two NMT2 isoforms have the in vitro capacity to catalyze the triple methylation of PEA to produce PCho, but with different efficiencies.

As an independent approach to confirm this unexpected result, we next tested the ability of NMT2.1 and NMT2.2 to rescue the *pem1*Δ *pem2*Δ Cho auxotroph yeast mutant, as has been shown for the biochemically verified spinach (*Spinacia oleracea*) PEAMT (Nuccio et al., 2000), wheat (*Triticum* sp.) PEAMT1 (Charron et al., 2002), and Arabidopsis NMT1 and NMT3 (Chen et al., 2018). Consistent with our NMR data, expression of either NMT2.1- or NMT2.2-enabled *pem1*Δ *pem2*Δ cells to grow (Fig. 3, A–C). However, while NMT2.2 expressing cells grew fast and independently of exogenous ethanolamine (EA) supply to the growth media, NMT2.1 cell growth on the contrary showed a strong dependence on EA supply (Fig. 3, B and C). However, under prolonged incubation, some growth eventually occurred even in the absence of EA supplementation (Fig. 3C). All transgenic cells, whether expressing NMT2.1 or NMT2.2, showed similar growth when supplied with methylethanolamine (MEA) or Cho (Fig. 3A). As a whole, these results concur to show that both NMT2 isoforms have the ability to catalyze the three step-wise methylations of PEA to form PCho, but that NMT2.2 is much more efficient than NMT2.1 in using PEA as a substrate.

To assess the physiological significance of that difference in the catalytic properties of the two NMT2 enzymes, we individually expressed the *NMT2.1* and *NMT2.2* cDNAs in the phosphocholine-deficient *nmt1* mutant, under the control of the *NMT1* promoter. We

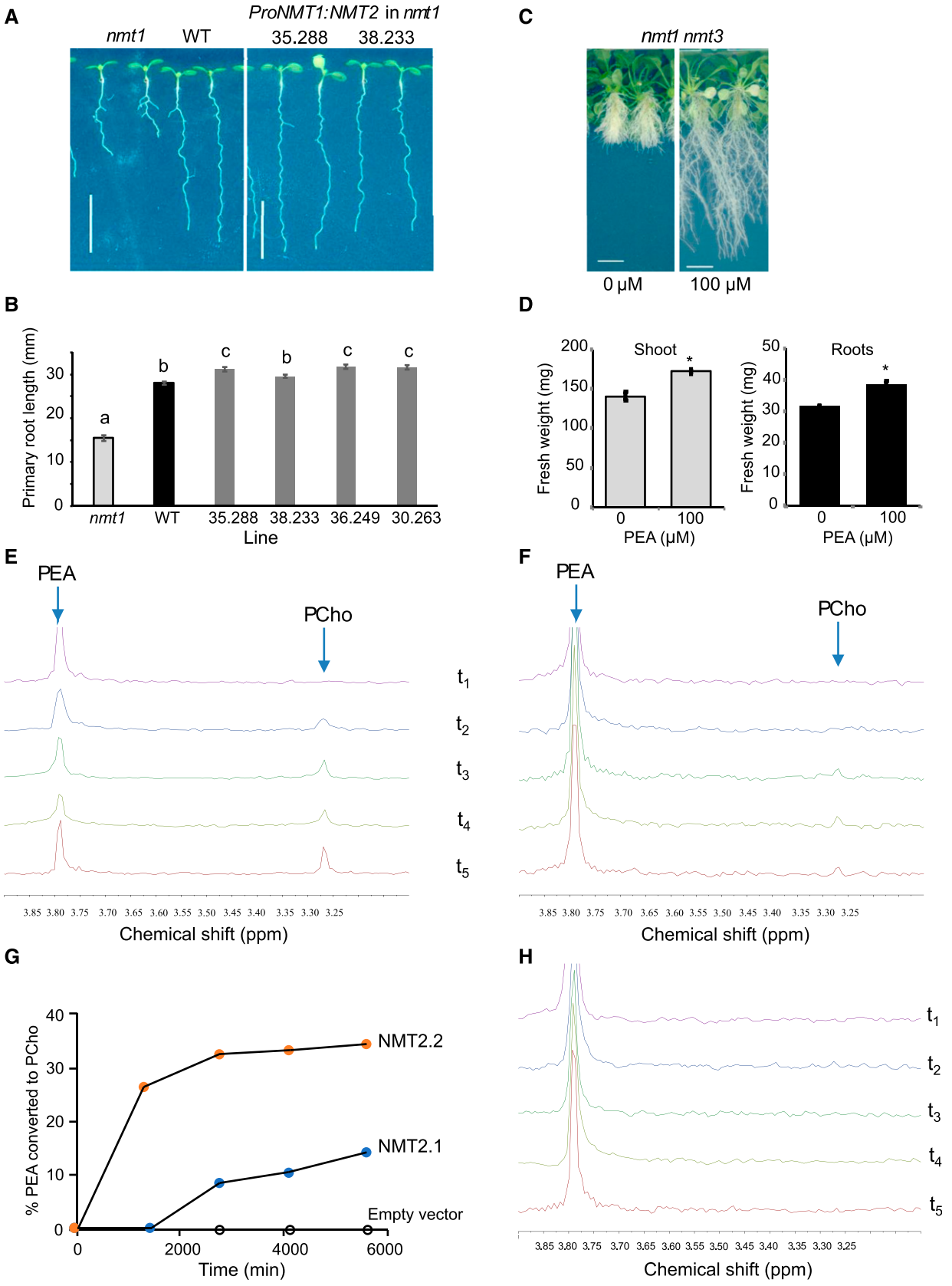
A
ProNMT1:NMT2 in nmt1
nmt1
WT
35.288
38.233
C
nmt1 nmt3
0 µM
100 µM
B
Primary root length (mm)
a
b
c
b
c
c
nmt1
WT
35.288
38.233
36.249
30.263
Line
D
Shoot
Roots
Fresh weight (mg)
PEA (µM)
E
PEA
PCho
t1
t2
t3
t4
t5
Chemical shift (ppm)
F
PEA
PCho
Chemical shift (ppm)
G
% PEA converted to PCho
NMT2.2
NMT2.1
Empty vector
Time (min)
H
t1
t2
t3
t4
t5
Chemical shift (ppm)

examined complementation of the *nmt1* mutant's distinctive root developmental defects (Cruz-Ramírez et al., 2004; Chen et al., 2018). The *NMT2.2* transgene restored normal root development (Fig. 4, A and B). In contrast, roots expressing *ProNMT1:NMT2.1* looked similar to *nmt1* roots. Only when PEA was exogenously supplied was partial rescue observed (Fig. 4B). This result shows that the NMT2.1 enzyme has the capacity to methylate PEA in planta, but with much less efficiency than NMT2.2. It is likely a minor contributor to the formation of MEA and PCho in the physiological range of EA concentrations.

NMT2 Is Not Totally Redundant Physiologically

To better understand the physiological functions of the two NMT2 isoforms, we isolated homozygous *nmt2* mutants from two independent T-DNA insertion lines: SALK_204065C and the previously characterized SALK_006037 (BeGora et al., 2010). Only the former, SALK_204065C, was confirmed as a *nmt2* knock-out mutant lacking expression of both *NMT2.1* and *NMT2.2*, and thus was used in further experiments. The homozygous progeny of SALK_006037 consistently showed *NMT2* expression in our hands, and in fact at higher levels than in the wild type background (Supplemental Figure S2). Under further examination, it appeared that the T-DNA insertion in that line is in the 5′UTR of the gene, while the SALK_204065C allele carries a T-DNA in exon 2, precluding transcription of both *NMT2.1* and *NMT2.2*.

SALK_204065C seedlings (hereafter referred to as *nmt2*) showed no difference to the wild type when grown on solid media (Fig. 5, A and B). Moreover, introducing the *nmt2* mutation into the *nmt1* or *nmt3* backgrounds had no overt effect on vegetative growth. The *nmt1 nmt2* and *nmt2 nmt3* seedlings showed similar lipid profiles to *nmt1*, *nmt3*, or the wild-type seedlings, unlike the *nmt1 nmt3* mutant, with no significant difference in either the total concentrations of PC or other major phospholipids or the concentrations of individual molecular species (Supplemental Figure S3; Supplemental Figure S4, A–H). The only detectable variation in lipid composition was an increased triacylglycerol (TAG) content in *nmt1 nmt2* roots. When transferred to soil, single mutants and *nmt1 nmt2*, and *nmt2 nmt3* mutants still showed similar growth and developmental phenotypes to the wild-type, apart from some reduction in stem elongation and mature height in the *nmt1 nmt2* mutant (Fig. 5, C–H, and N–S). However, similar yields were achieved. In light of the extreme dwarfism of the *nmt1 nmt3* mutant, its slow and impaired development (Fig. 5, I and T), and its severely reduced synthesis of PC (Supplemental Figure S3; Chen et al., 2018), these data indicate a minor role of NMT2 compared to NMT1 and NMT3 in the maintenance of PC homeostasis and normal Arabidopsis development.

NMT2 Loss of Function in a *nmt1 nmt3* Background Precludes PC Synthesis and Is Lethal

We wished to find out whether NMT2 activity could, nevertheless, at least partially account for the significant residual PC synthesis occurring in *nmt1 nmt3* seedlings and associated developmental defects. We introduced the *nmt2* loss-of-function mutation into the *nmt1 nmt3* mutant. The *nmt1 nmt2 nmt3* seeds germinated; newly germinated seedlings contained some PCho and PC (Fig. 6, A–C), but at much reduced level compared to the wild-type seedlings (43% and 30% decrease of radicle and cotyledon PC content, respectively). Consistently the levels of Cho, which in plants can be produced through dephosphorylation of PCho or hydrolysis of PC (Summers and Weretilnyk, 1993; McNeil et al., 2000; Welti et al., 2002), were also reduced. These *nmt1 nmt2 nmt3* seedlings did not progress beyond the unfolded cotyledon stage. The

Figure 1. (*Continued.*)
NMT2 encodes two PEAMT isoforms with different catalytic properties. A–B, Complementation of the *nmt1* mutant by *ProNMT1:NMT2*. A, Representative photographs of 8-d-old *nmt1*, the wild-type (WT), and *nmt1* transgenic seedlings expressing *NMT2* under the control of the *NMT1* promoter; T3 homozygous seedlings of two independent lines 35.288 and 38.233 are shown. B, Primary root lengths for *nmt1*, the wild type, and four independent ProNMT1:NMT2 lines. Means ± SE, $n = 25$ to 28. Scale bar is 1 cm. Values with different letters are significantly different by one-way ANOVA followed by posthoc test ($P < 0.05$). C–D, Complementation of the *nmt1 nmt3* mutant defective growth by exogenous PEA supply. Representative photographs (C) and shoot and root fresh-weights (D, means ± SE, $n = 8$) of 7-wk-old seedlings germinated on solid media (1.2% agar with 1/2 MS and 1% Suc) in the presence of 0 or 100 μM PEA. Seedlings were transferred to fresh plates on day 7 and every two weeks thereafter. Scale bar is 1 cm. The * in (D) indicate statistical significance by Student *t* test ($P < 0.05$). E and F, NMT2.1 and NMT2.2 can form PCho from PEA. Conversion of PEA to PCho was monitored by ^{31}P-NMR in protein extracts of equal concentrations from yeast cells expressing NMT2.2 (E) and NMT2.1 (F), over a time course of 94 h. Spectra were recorded 5 to 9 min (t_1) after initiation of the reactions through the addition of substrates PEA and S-Adenosyl methyl donor, and daily thereafter (t_2 to t_5). G, Conversion rates of PEA to PCho in protein extracts of equal concentrations, from cells expressing NMT2.1 and NMT2.2. Integrals for ^{31}P-NMR resonances were measured at 3.79 ppm (PEA) and 3.27 ppm (PCho) and were quantified against methylphosphonate (23.48 ppm) as an internal standard. Equal volumes of methylphosphonate and PEA solutions were added at starting concentrations of 5 mM and integrations are arbitrarily set to 100. As the reaction progresses a rise in PEA conversion to PCho is observed, theoretically reaching a value of 100% for full conversion.H, Absence of PCho in NMR spectra from reactions with protein extracts from cells expressing the empty vector, at any time point.

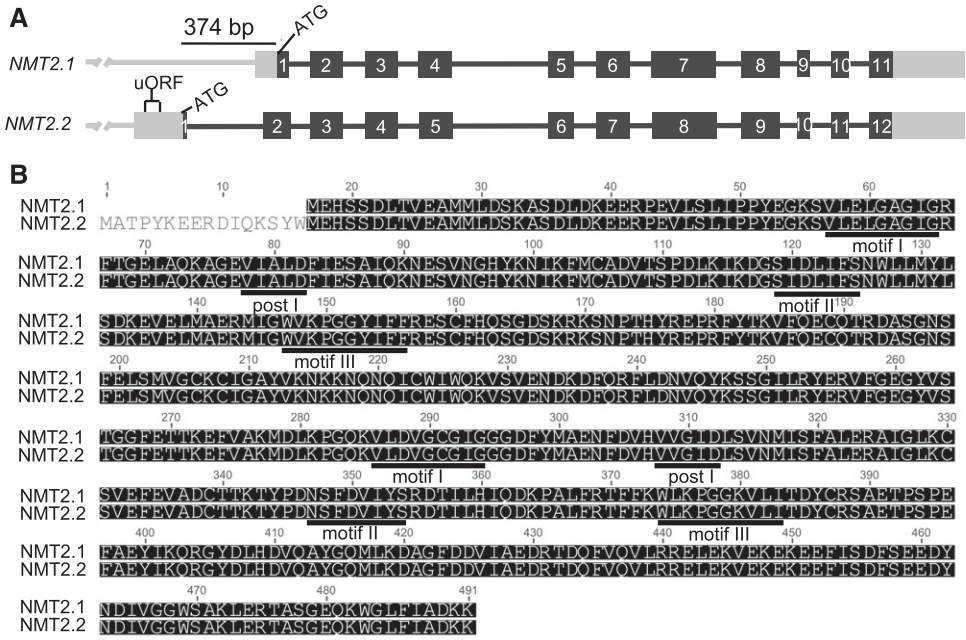

Figure 2. Intron-exon structure of *NMT2.1* and *NMT2.2* and alignment of the encoded proteins. A, Schematic representation of *NMT2* gene structure. Gray boxes indicate UTRs; gray lines indicate promoters. Black boxes indicate exons, numbered 1 to 11 in *NMT2.1*, and 1 to 12 in *NMT2.2*. Black lines represent introns. The upstream open reading frame (uORF) of *NMT2.2* is indicated. The 374 bp difference at the N-terminal end of the two transcripts is also indicated. B, Alignment of NMT2.1 and NMT2.2 deduced amino acid sequences. The alignment was made using ClustalW built in Geneious v7.1.3 (Biomatters) with default parameters (scoring matrix, Blosum; gap open cost, 10; gap extend cost, 0.05). The four typical motifs of the N- and C-terminal catalytic domains of PEAMTs are indicated.

cotyledons quickly became chlorotic and died (Fig. 5I). Supplementation of Cho from germination recapitulated the wild-type growth and development (Fig. 5, K and L, compared to Fig. 5, C and M; Supplemental Figure S5), thus showing that the CDP-Cho pathway was fully functional in these seedlings. Death was the result of Cho deficiency due to disruption of the phospho-base methylation pathway. We hypothesized that germination and cotyledon unfolding likely relied on stored PC of maternal origin. To test this idea, 7-day-old *nmt1 nmt2 nmt3* seedlings with just unfolded, fully green cotyledons, were fed labeled ^{13}C-ethanolamine, alongside *nmt1 nmt3* and the wild-type seedlings as controls. The formation of labeled PC was monitored by mass-spectrometry over an 8-h period (Fig. 6D). No net PC synthesis from labeled ethanolamine could be detected in the triple mutant, contrary to the wild-type or, to a lesser extent, the *nmt1 nmt3* mutant. To confirm this result was not due to general metabolic failure in *nmt1 nmt2 nmt3* seedlings, we concurrently monitored the formation of labeled PE. ^{13}C-PE synthesis proceeded at similar rates in *nmt1 nmt2 nmt3* seedlings as in *nmt1 nmt3* or the wild-type seedlings (Fig. 6E). Taken together, these data demonstrate that NMT2 activity fully accounts for residual de novo PC synthesis in the *nmt1 nmt3* mutant, and that NMT2 activity is absolutely required for plant survival in the absence of functional NMT1 and NMT3.

Specificity in the Expression and Transcriptional Regulation of *NMT2.1* and *NMT2.2*

We examined *NMT2* gene expression to better understand how *NMT2* function (alone) was able to sustain de novo PC synthesis and the formation of some viable vegetative and reproductive organs. We used transcript-specific primers to separately quantify *NMT2.1* and *NMT2.2* mRNAs using quantitative polymerase chain reaction (qPCR). *NMT2.1* expression was present in young seedlings, at levels comparable to *NMT1*, and was also present in expanding rosette or cauline leaves, but it was weak in mature leaves and flowers (Fig. 7A; Supplemental Figure S6). In contrast, *NMT2.2* was found to be preferentially expressed in floral buds and open flowers, at levels higher or similar to *NMT2.1*. Unexpectedly, *NMT2.2* expression elsewhere was at least an order of magnitude lower than *NMT2.1* expression, and down to noise levels in mature rosette or cauline leaves.

These results indicated specificity in spatial expression patterns between *NMT2.1* and *NMT2.2*. To examine this situation in more detail, we fused the putative *NMT2.1* and *NMT2.2* promoter fragments with the β-glucuronidase (*GUS*) reporter gene (Supplemental Figure S6, B and C). Two transcripts can be produced from the *ProNMT2.1:GUS* transgene, as there are two TSS. But the transcript produced from TSS2 cannot be translated into a functional GUS protein, because the

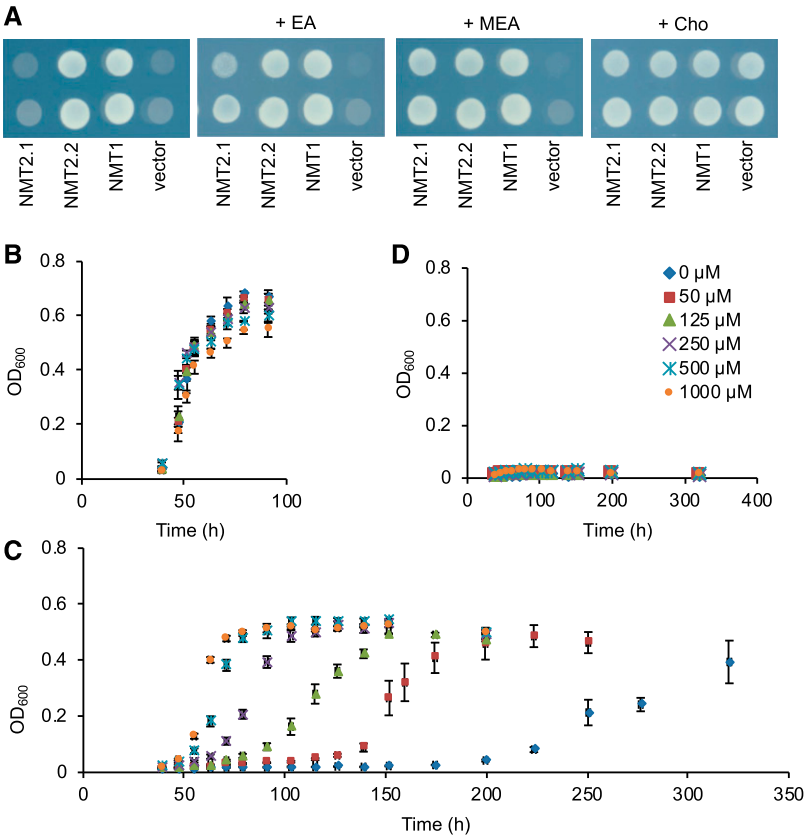

Figure 3. NMT2.1 and NMT2.2 differ in their ability to complement the Cho auxotroph yeast mutant *pem1*Δ *pem2*Δ. A, Yeast mutant strain *pem1*Δ *pem2*Δ expressing Arabidopsis *NMT2.1*, *NMT2.2*, and *NMT1* or the empty vector as positive and negative controls, respectively, were grown on agar supplemented with minimal media and 2% (w/v) Gal, and 1-mM Cho or ethanolamine (EA) or monomethylethanolamine (MEA), as indicated, at 37°C for 4 d. The two rows show replicated spots. B to D, Yeast *pem1*Δ *pem2*Δ cells harboring *NMT2.2* (B), *NMT2.1* (C), or empty vector (D) were initially grown in liquid minimal media supplemented with 1-mM Cho and 2% (w/v) Glc to the exponential phase. Cells were then washed with sterile water and diluted into minimal media supplied with 2% (w/v) Gal and the indicated concentrations of EA, and incubated at 28°C. Samples were taken over two weeks at the indicated times after the start of incubation under inducing conditions ($t = 0$) for measurements of optical density (OD_{600}) using LabSystems Multiskan RC. Values are ± SE ($n = 4$).

first start codon in that transcript is not in frame with the start codon of the *GUS* gene. *ProNMT2.1:GUS* lines displayed clear staining in leaf primordia, progressively fading during blade expansion, except along veins where strong GUS expression was visible throughout development (Fig. 7, B and C). In roots, the vasculature was also strongly stained, as well as the columella and quiescent center (Fig. 7, D–F). In contrast, *NMT2.2* promoter activity was only detected in the root columella but not the quiescent center or vasculature, and in addition was very faint (to nondetectable) in leaves (Fig. 7, G–K). Observations of reproductive organs confirmed the largely nonoverlapping patterns of the two *NMT2* transcripts (Fig. 7, L–Y). *NMT2.1* promoter activity was present in mature pollen and along the stamen's filament, being intense at its anchor point to the flower receptacle (Fig. 7, M and N), and it also was found along the silique's septum and ovules funiculus (Fig. 7U). In contrast, NMT2.2 promoter activity was confined to pollen. As a whole, these results reveal a more specific and restricted expression of *NMT2.2* than *NMT2.1*. They also show that alternate use of the promoter in the transcription of *NMT2* is developmentally regulated and involves cell- and tissue-specific controlling mechanisms.

The promoter sequences used for the *ProNMT2.1:GUS* and *ProNMT2.2:GUS* reporters were identical except for an additional 374 bp at the 3′ end of the *NMT2.1* construct (Supplemental Figure S6, B and C). This fragment spans from the ATG start codon of *NMT2.2* to the nucleotide preceding the ATG start codon of *NMT2.1*. To investigate its role in the stark difference between *NMT2.1* and *NMT2.2* expression patterns, we fused it with *GUS* (Supplemental Figure S6D). To overcome the possible translation from the ATG at the beginning of the fragment, we excluded the first nucleotide A from the construct. Transgenic lines showed clear GUS staining in the vasculature of the root and leaves, and in the quiescent center, similar to the *proNMT2.1:GUS* lines (Fig. 7Z compared to Fig. 7, B–F; Supplemental Figure S6, E and F). These data indicate that the broader expression of *NMT2.1* compared to *NMT2.2* is controlled by that 374 bp promoter region.

There is apparently very low expression of *NMT2.2*, except in a few limited domains. Yet it has (alone) a capacity to enable sufficient PC synthesis for survival of the *nmt1 nnmt3* mutant and the formation of some reduced but viable organs of all types. We thus reasoned that *NMT2.2* expression might be enhanced in the absence of the other *NMT*s compared to its constitutive expression in the wild type. To test this idea, we measured *NMT2.1* and *NMT2.2* transcript abundance in the *nmt1*, *nmt3,* and *nmt1 nmt3* backgrounds (Fig. 8, A and B). *NMT2.1* expression was unaffected by the presence or absence of functional *NMT1* or *NMT3*, or both. On the contrary, *NMT2.2* expression showed a 4.4- and 6.2-fold increase in *nmt1 nmt3* roots and shoot, respectively, compared to the wild type, and also increased in the two single mutants. These data support the shared biochemical function of NMT2.2 with NMT1 and NMT3

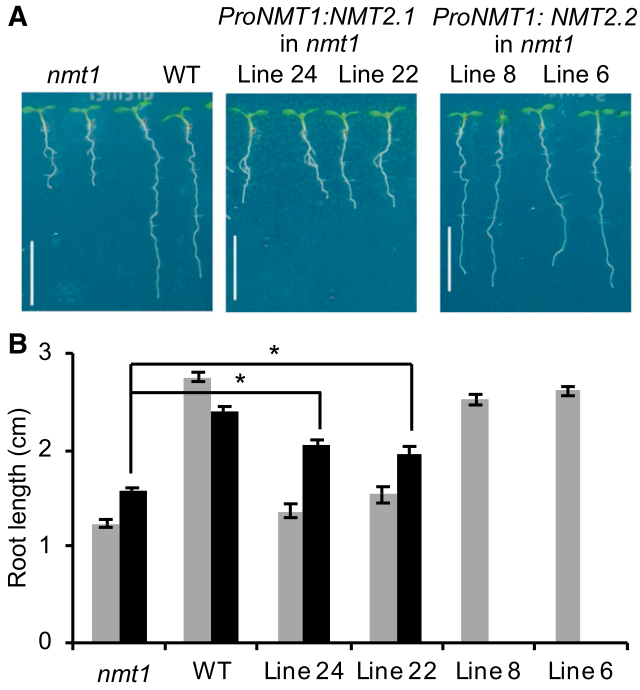

Figure 4. Complementation of the *nmt1* mutant short root phenotype by *NMT2.2*. A, Representative seedlings of *nmt1*, the wild type, and homozygous transgenic lines expressing *NMT2.1* or *NMT2.2* under the control of the *NMT1* promoter (lines 24 and 22; and lines 8 and 6, respectively). Seedlings were grown on one-half MS media supplemented with 1% Suc for 8 d. Scale bars are 1 cm. B, Primary root lengths measured on day 8 for seedlings grown on 0-mM PEA (gray bars) or 1-mM PEA media (black bars). Bars represent mean values ± SE (n = 16 to 32 seedlings). The * indicate statistically significant genetic differences for PEA-fed ProNMT1:NMT2 seedlings compared to the wild-type by Student's t test ($P < 0.05$).

as a PEAMT catalyzing the three step-wise methylations of PEA to form PCho.

NMT1 is known to be sensitive to end-product feedback inhibition at the transcriptional and translational level through regulatory mechanisms involving its uORF (Tabuchi et al., 2006; Alatorre-Cobos et al., 2012). Would *NMT2.2* have that property also? This possibility was suggested by the partial compensation of loss of *NMT1* and *NMT3* function by enhanced expression of *NMT2.2* and the presence of a uORF in the 5′UTR of NMT2.2, identical to NMT1's uORF. To investigate, we carried out Cho feeding assays (Fig. 8C). Cho supplementation caused a significant reduction of *NMT2.2* expression, and also of *NMT1*, while *NMT2.1* expression was unaffected. This result further supports functional homology between *NMT2.2* and *NMT1* and functional divergence from NMT2.1, involving the uORF.

NMT2 Function Maintains Pollen Competitiveness in the Absence of Functional *NMT1* and *NMT3*

We reported earlier that *NMT1* is haplo-insufficient for normal development of the *nmt1 nmt3* seed progeny of selfed *nmt1+/− nmt3* flowers (Chen et al., 2018). Embryogenesis in *nmt1 nmt3* segregating seeds within *nmt1+/− nmt3* siliques is impaired, particularly in the basal embryo domain, and morphogenesis is often prematurely arrested, so that the seed shrivels and aborts or remains nonchlorophyllic. We took advantage of these distinct phenotypes to investigate the consequences of totally suppressing the P-methylation pathway on seed development and viability. We introduced the *nmt2* mutation in the *nmt1+/− nmt3* background. Contrary to expectations, as a whole, *nmt1 +/− nmt2 nmt3* siliques exhibited fewer abnormal seeds than *nmt1+/− nmt3* siliques, 13.9% compared to 24.2%, respectively, of white and flat, or brown small seeds. Moreover, most of these seeds were in the silique's upper half (Table 1; Fig. 9C). Their frequency there was not significantly different from 25% (23.2%; Table 1), indicating that these seeds corresponded to triple mutant homozygous *nmt1 nmt2 nmt3* seeds. Seed clearing revealed that they contained nonviable embryos, a few clearly arrested at the globular to early torpedo stages, but most presenting as a totally unrecognizable amorphous mass of cells within the seed cavity (Fig. 9, I and K). Such an extreme impairment of embryogenesis was not found in *nmt1 nmt3* seeds (Fig. 9, E–G). This result indicates that embryogenesis cannot proceed without minimum PEAMT activity and PC synthesis in the seed itself.

Intrigued by the nonrandom spatial distribution of homozygous triple mutant seeds in *nmt1+/− nmt2 nmt3* siliques, we reasoned that it could reflect either a nonrandom distribution of *nmt1 nmt2 nmt3* ovules or a nonrandom fertilization success rate by *nmt1 nmt2 nmt3* pollen. To test these hypotheses, we performed reciprocal crosses of *nmt1+/− nmt2 nmt3* and the wild-type flowers. We genotyped the F1 progeny, separating seeds of the siliques' top and bottom halves. When the wild-type was used as the male parent, *nmt1+/− nmt2 nmt3* and *nmt2 nmt3* seeds were found in similar proportions in the silique's upper and lower halves (Table 2; 58% and 63%), indicating a spatially unbiased distribution of the *nmt1 nmt2 nmt3* female gametophyte genotype. However, when *nmt1+/− nmt2 nmt3* flowers were used as pollen donors and the wild-type was used as the female parent, the *nmt1* allele was found at a frequency of 57.1% (insignificantly different from 50%) among seeds of the silique's top half, but only 18.6% among seeds of the bottom half (Table 2). These results show that the nonrandom distribution of *nmt1 nmt2 nmt3* seeds in the *nmt1+/− nmt2 nmt3* silique is of male origin. They suggest that triple mutant *nmt1 nmt2 nmt3* pollen tubes initially elongate at a similar rate as *nmt2 nmt3* double mutant pollen tubes and also have similar fertilization success rates, but then slow down or stop growing, so that most ovules lower down along the silique get fertilized by *nmt2 nmt3* male gametes rather than *nmt1 nmt2 nmt3* gametes. We earlier showed that *nmt1*, *nmt3*, or *nmt1 nmt3* pollen had

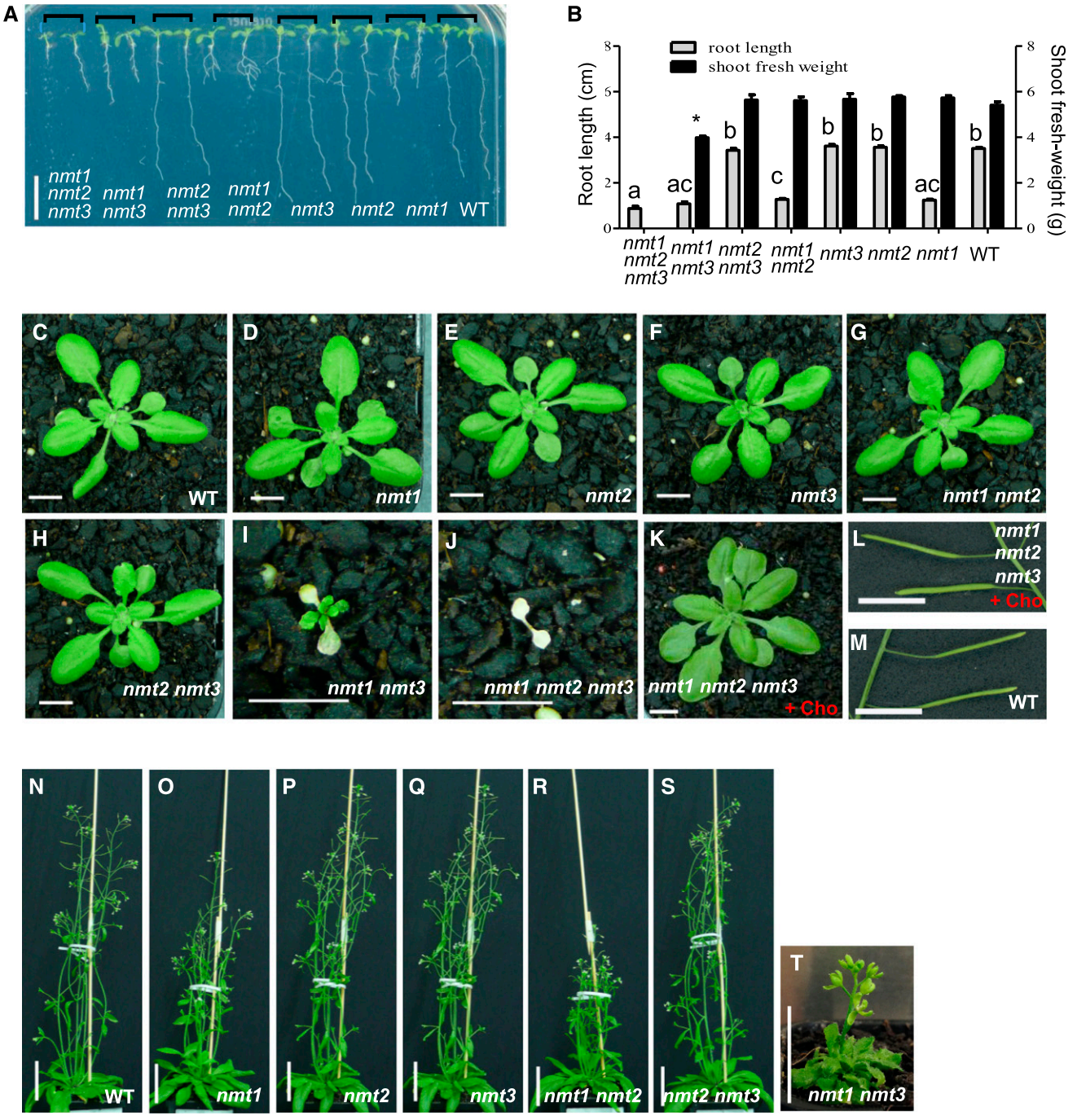

Figure 5. Developmental phenotypes induced by the *nmt2* loss-of-function mutation. A, Representative photographs of the wild type and all *nmt1, nmt2, nmt3* mutant combinations, including the triple knock-out mutant *nmt1 nmt2 nmt3*. Ten-day-old seedlings grown on 1/2 MS with 1% Suc. Scale bar is 1 cm. B, Primary root length and shoot fresh-weights (gray and black bars, respectively). Means ± SE ($n = 28$ to 30 for root lengths; $n = 4$ pools of 8 to 32 seedlings, depending on genotype, for shoot fresh-weights). Statistically significant genetic differences in root lengths ($P < 0.05$) are denoted by different letters above the gray bars. The asterisk denotes the only significant difference in shoot fresh-weight among lines (shorter lengths in the *nmt1 nmt3* mutant compared to all other lines). C–I, Pictures of the 3-wk-old wild type, *nmt1*, *nmt2*, *nmt3*, *nmt1 nmt2*, *nmt2 nmt3*, *nmt1 nmt3*, and *nmt1 nmt2 nmt3* plants grown in soil. K and L, Rescue of vegetative and reproductive development of the *nmt1 nmt2 nmt3* mutant by choline (Cho). Pictures show 3-wk-old *nmt1 nmt2 nmt3* rosettes (K) and fully elongated 10-d-old siliques (L) from plants sprayed daily with 2-mM Cho, starting 4 d postgermination. M, Wild type siliques shown for comparison, at the same magnification. C–M, Scale bars are 1 cm. N–T, Pictures of 8-wk-old reproductive plants of the wild type and *nmt1*, *nmt2*, *nmt3*, *nmt1 nmt2*, *nmt2 nmt3*, and *nmt1 nmt3* mutants. Scale bars are 2.5 cm for the *nmt1 nmt3* mutant and 5 cm for all other lines.

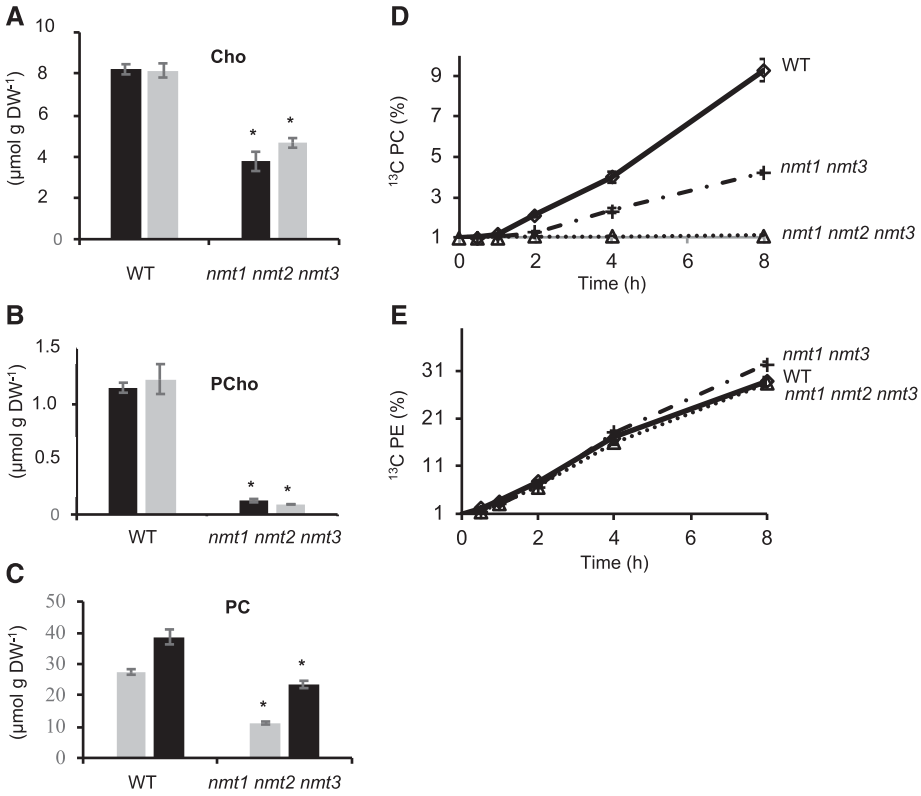

Figure 6. Loss of *NMT2* in the *nmt1 nmt3* double knock-out mutant abolishes de novo PC synthesis. A to C, Concentrations of Cho (A), PCho (B), and PC (C) in the wild type and *nmt1 nmt2 nmt3* newly germinated seedlings 7 d after sowing (black bar: shoot; gray bar: root). Means ± SE (n = 5 to 6 pools of 30 to 40 seedlings). The * indicates significantly lower values in mutant than wild-type tissue (root, or shoot) by Student's t test for each tissue ($P < 0.01$). D and E, Incorporation of ^{13}C-ethanolamine into PC and PE. Time course of ^{13}C-PC (D) and ^{13}C-PE (E) incorporation in the wild type, *nmt1 nmt3* and *nmt1 nmt2 nmt3* plants, expressed as % of total PC. 7-d-old seedlings grown on 1.2% agar with 1/2 MS and 1% Suc were transferred to 1/2 MS and 1% Suc liquid media supplemented with 250 μM of ^{13}C-ethanolamine. Samples were harvested at the indicated times for measurements of ^{13}C incorporation in PC and PE. Values shown are means ± SE (n = 6). Genotypic differences in (D) are highly significant ($P < 0.001$) by Student's t test; differences in (E) are all nonstatistically different.

similar fertilization success rates, also similar to the wild-type (Chen et al., 2018). Our results here indicate that loss of the whole NMT family compromises pollen tube growth, thus implying that this process requires a minimum amount of locally synthesized PC.

Critical Amino Acids for PEAMT Activity

Given the vital necessity of PEAMT activity for PC synthesis, survival, and normal development, we took advantage of the high sequence similarity between the two NMT2 isoforms to investigate what could determine their differential capacity to catalyze the committing step of the phospho-base methylation pathway. The only difference between the deduced amino acids (AAs) of NMT2.1 and NMT2.2 is the presence of 16 additional AA at the N-terminal end of the latter. Out of these 16 AAs, five are highly conserved across all demonstrated phosphoethanolamine methyl transferases from plants and algae (Fig. 10A). Of these, three are also conserved in the parasitic nematode *Haemonchus contortus* HcPMT1 and in the *C. elegans* CePMT1, both of which can also catalyze the methylation of PEA to PCho. We thus hypothesized that these conserved AAs might be essential to PEAMT activity. To test this, we created NMT2.2 mutant variants in which either E8, R9, K13, Y15, or W16 were mutated to Ala, and we expressed them in the *pem1*Δ *pem2*Δ Cho auxotroph yeast mutant. Each of these mutations abolished the ability of the native NMT2.2 to rescue mutant yeast cell growth on minimal media or media supplemented with EA after 2 d of growth (Fig. 10B). After 4-d incubation on minimal media, cells expressing E8A and K13A protein variants had grown. But those expressing R9A, Y15A, and W16A still showed no growth (Fig. 10C). Supplementation of 1-mM EA enabled growth of all lines, but the growth of cells expressing the Y15A and R9A variants still lagged behind that of cells expressing the native NMT2.2, similar to the growth of cells expressing NMT2.1. These results identify R9, Y15, and W16 as key residues for the PEAMT activity of NMT2.2 under physiological substrate concentrations, and to a lesser extent also E8 and K13. All cell lines grew similarly when exogenously supplied with MEA or Cho, at similar rates as control cells expressing NMT2.1, NMT2.2, or NMT1. This result shows that the catalytic importance of these key residues is specific to the first phospho-base methylation step converting PEA to PMMEA.

DISCUSSION

This study represents the characterization of a whole gene family encoding the phospho-base methylation branch of the plant PC biosynthetic pathway. The data presented show that Arabidopsis lacking the PEA methylation pathway is unable to synthesize the major phospholipid PC and is unable to survive, demonstrating that the methylation of PEA is the sole entry point for PC synthesis (Fig. 11). In addition, this study

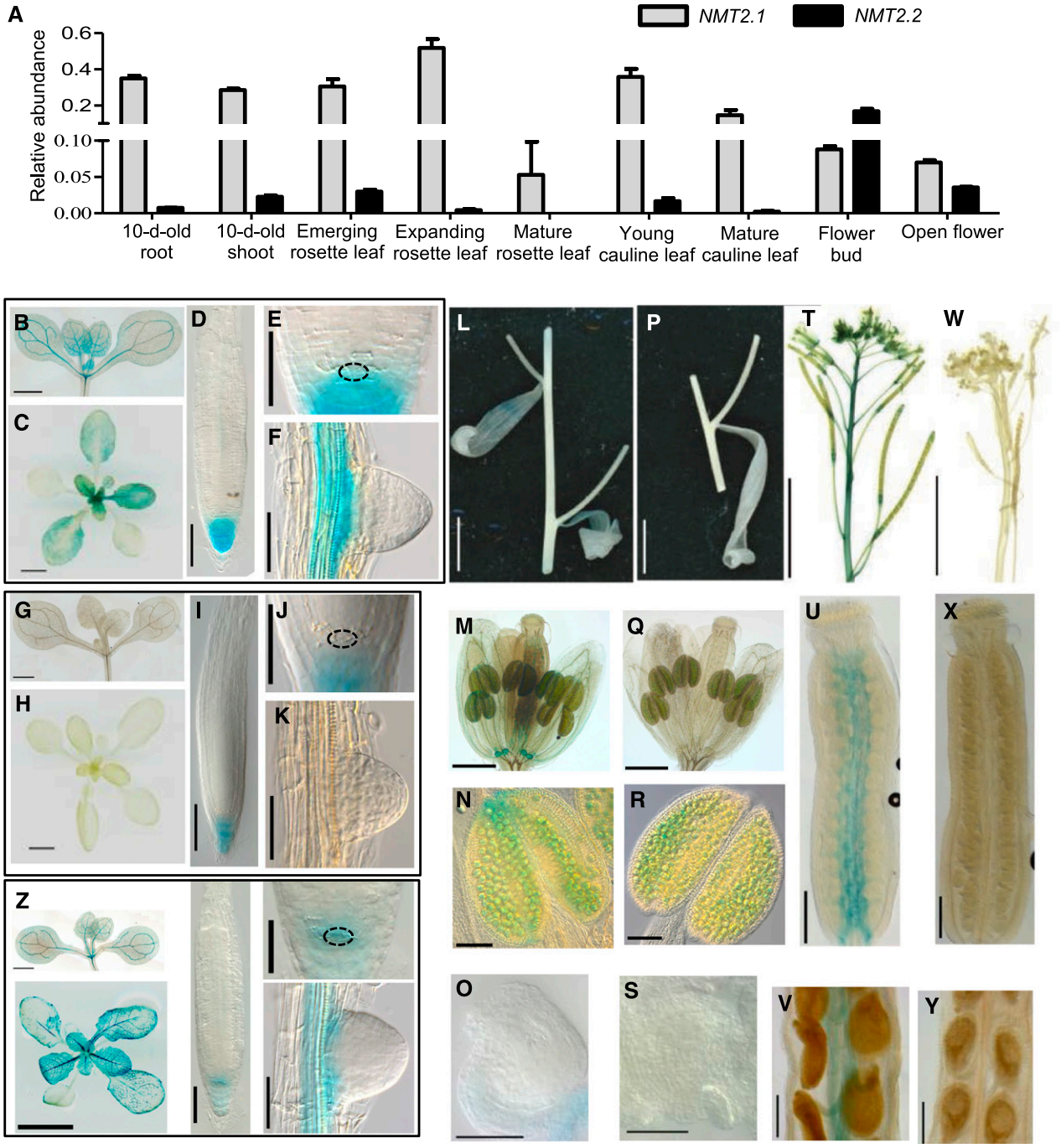

Figure 7. Transcript abundance and expression patterns of *NMT2* alternative transcripts *NMT2.1* and *NMT2.2*. A, Relative expression levels of *NMT2.1* and *NMT2.2* determined by RT-qPCR. *APT1*, *PDF2*, and *GAPDH* genes were used as reference genes. Values are means ± SE ($n = 4$ pools of organs from 3 to 20 plants depending on stages and organ). B to Z, GUS staining patterns in vegetative and reproductive tissues of wild-type plants harboring *ProNMT2.1:GFP:GUS* (B to F, L to O, T to V) or *ProNMT2.2:GFP:GUS* reporters (G to K, P to S, W to Y). Rosette (B and G), primary root (D, E and I, J), lateral root (F and K) of 10-d-old seedlings grown on agar plates; rosette of 18-d-old soil-grown plants (C and H); inflorescences (T and W); stage 12 flower (M and Q), anther (N and R), ovules (O and S), pistil (U and X), and seed funiculus (V and Y). The quiescent center is outlined by an oval dotted line in (E) and (J). Bars are 1 mm in (B) and (G), 50 μm in (E), (F), (J), (K), (O), and (S), 100 μm in (D), (I), (N), and (R), 200 μm in (U), (X), (V), and (Y), 2 cm in (T) and (W), 0.5 cm in (L) and (P), 500 μm in (M) and (Q), 1 cm in (C) and (H). Z, GUS staining patterns in *ΔProNMT2:GFP:GUS* shoot, primary root tip and lateral roots of 10-d-old seedling grown on agar plates; the rosette of 18-d-old soil-grown plants is also shown, for comparison to (B to F) and (G to K), at the same scales. The quiescent center of the primary root is indicated by the oval dotted line in (Z).

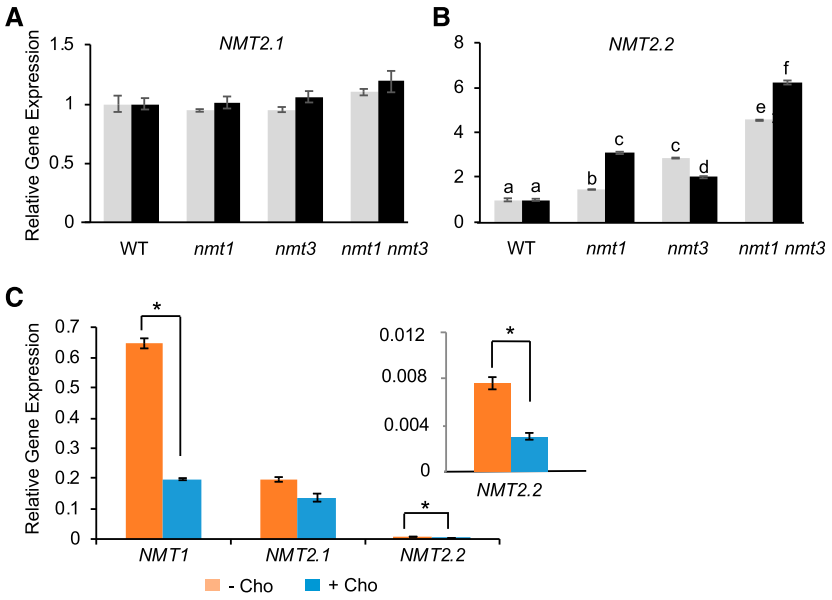

Figure 8. Differential sensitivity of *NMT2.1* and *NMT2.2* expression to NMT1 or NMT3 knock-out and Cho levels. A and B, Fold-change in *NMT2.1* and *NMT2.2* expression in *nmt1*, *nmt3* or *nmt1 nmt3* tissues compared to the wild type (the wild-type value was set to 1). The 10-d-old seedlings were grown on 1.2% agar with one-half MS and 1% Suc. Different letters denote statistically significant differences by two-way ANOVA ($P < 0.05$, $n = 4$ pools of 20 to 50 seedlings. C, Expression levels of *NMT1*, *NMT2.1*, and *NMT2.2* in wild-type seedlings grown on one-half MS with 1% Suc, 1.2% agar for 7 d, and then transferred to fresh media of the same composition or to media supplemented with 200-μM Cho for 2 d. The inset shows *NMT2.2* expression on an expanded scale. Values are means ± SE. The * indicate statistically significant expression differences for each gene, between Cho-fed and control seedlings by Student's *t* test, $P < 0.05$, $n = 4$ pools of 20 to 50 seedlings. Expression levels of target genes were normalized to the geometric mean of reference genes *AtAPT1*, *AtPDF2*, and *AtGAPDH*.

identifies critical amino acids for the ability of PEAMTs to catalyze that vital reaction.

Methylation of PEA Is the Sole Entry Point for De Novo PC Synthesis in Arabidopsis

Several interconnected routes have been identified for PC synthesis in plants. In this work we created an Arabidopsis *nmt1 nmt2 nmt3* knock-out mutant for the three closely related genes that have been implicated in the control of the phospho-base methylation pathway: two as genes encoding PEAMTs catalyzing the three sequential methylations of PEA both in vitro and in planta (Bolognese and McGraw, 2000; Lee and Jez, 2017; Chen et al., 2018), and the remaining one with unclear function (BeGora et al., 2010; Lee and Jez, 2017) and unknown physiological roles. We show that this mutant is lethal, unless seeds are fed Cho or phosphocholine (Fig. 5). The *nmt1 nmt2 nmt3* seeds can only recover under continuous Cho feeding. These seeds germinate, but postembryonic development cannot proceed in the absence of exogenous Cho supply. Through chase experiments with exogenously supplied labeled EA, and metabolite profiling, we demonstrate that the *nmt1 nmt2 nmt3* mutant is incapable of de novo PC synthesis from PEA (Fig. 6). This incapability shows that *NMT2* function fully accounts for the residual PC synthesis present in the *nmt1 nmt3* double mutant, and the mutant's ability to acquire autotrophic growth.

The formation of PE in the *nmt1 nmt2 nmt3* mutant is not affected at these early seedling stages (Fig. 6E).If PC could be synthesised by direct methylation of PE as in mammals and yeast, and/or by methylation of PE-derived LysoPE to form LysoPC followed by re-acylation to form PC as proposed by Liu et al. (2015), or by some other means, we would expect some PC

Table 1. *Frequency of abnormal seeds (pale green, white or brown) in* nmt1+/− nmt2 nmt3 *and* nmt1+/− nmt3 *siliques*

Mutant	No. of Seeds Examined	Frequency of Abnormal Seeds (%) Along Silique		Ratio of Frequencies Top Half/Bottom Half	χ^2 Value	*P* Value
		Top Half	Bottom Half			
nmt1+/− nmt2 nmt3	1,792	23.2	4.4[a]	5.3[b]	110.2	<0.001
nmt1+/− nmt3	1,196	24.9	23.5	1.1	0.28	0.60

[a]Frequency significantly different from expected 25% frequency. [b]Ratio significantly different from expected 1:1 ratio for random distribution, $P < 0.001$.

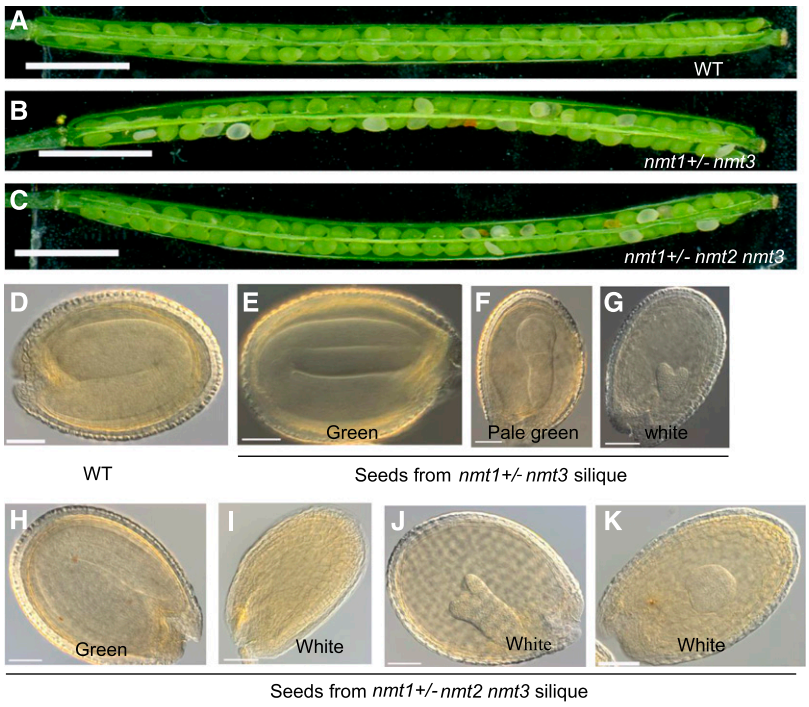

Figure 9. Loss of NMT2 in *nmt1+/−nmt3* siliques modifies the distribution of *nmt1 nmt2 nmt3* seeds and aggravates embryo developmental defects. A to C, Dissected silique of wild-type (A), *nmt1+/− nmt3* (B), and *nmt1+/− nmt2 nmt3* (C) inflorescences showing normal, swollen green seeds; pale green to white seeds; small brown seeds. Shown are 10-d-old siliques. Scale bars are 2.5 mm. D to K, Cleared seeds from wild-type silique (D), *nmt1+/− nmt3* silique (E to G), *nmt1+/− nmt2 nmt3* silique (H to K), showing normal mature embryos (D, E, H); and delayed, arrested, or totally impaired embryos (F, G, J, and I, K, respectively). Seed color is indicated within (B to K). Scale bars are 100 μm.

synthesis to still occur. This is not the case. Our data therefore provide evidence that (a) the phospho-base methylation pathway is the sole entry point for PCho and PC production in Arabidopsis in the absence of exogenous free Cho; (b) that it is controlled by three genes, *NMT1*, *NMT2*, and *NMT3;* and (c) that the process is vital (Fig. 11).

PC Is Absolutely Required for Survival

The importance of PC for plant development was shown by the abnormal root development of *NMT1* loss-of-function mutants *nmt1* and *xpotl1*, despite only slightly decreased total PC concentrations and subtle changes in the profiles of PC molecular species (Cruz-Ramírez et al., 2004; Chen et al., 2018). When PC synthesis was further compromised by knocking out *NMT3* in the *nmt1* mutant, multiple aspects of vegetative and reproductive development were affected, and extreme dwarfism and extensive sterility were observed, concomitantly with profound alterations of lipid composition (Fig. 5; Supplemental Figure S3 and Supplemental Figure S4; Chen et al., 2018). Yet, some viable organs could be formed, and the developmental cycle could ultimately unfold until completion, despite cells being unable to maintain homeostatic levels of PC. Whether PC synthesis is absolutely required for plant survival was unknown. The creation of a triple mutant *nmt1 nmt2 nmt3* and total knock-out for de novo synthesis enabled us to answer that question. The inability of *nmt1 nmt2 nmt3* seedlings to establish autotrophic growth and progress past the cotyledon stage demonstrates that PC is absolutely necessary for plant survival, and that their germination relied on PC of maternal origin, stored during seed maturation on the mother plant, essentially in the embryo—this is where most of the seed reserves are located in Arabidopsis (Baud et al., 2008).

Requirement of PC synthesis for survival was also observed in other organisms using mutants of enzymes catalyzing the phospho-base methylation pathway, such as *pmt1* and *pmt2* in *C. elegans* and *PfPMT* in *P. falciparum*. RNAi silencing of the *C. elegans pmt-1* or

Table 2. *Frequency of F1 seeds containing the* nmt1 *allele in siliques from reciprocal crosses of* nmt1+/− nmt2 nmt3 *and the wild-type flowers*

Cross	No. of Seeds Genotyped	Silique Half	Frequency of Seeds Containing the *nmt1* Allele[a] (%)	Top Half to Bottom Half Ratio of Seeds Containing the *nmt1* Allele[b]
nmt1+/− nmt2 nmt3 ♀ X WT ♂	91	top	58.2 (0.14)	0.9
nmt1+/− nmt2 nmt3 ♀ X WT ♂	95	bottom	63.2 (0.01)	
WT♀ X *nmt1+/− nmt2 nmt3* ♂	105	top	57.1 (0.17)	3.1
WT♀ X *nmt1+/− nmt2 nmt3* ♂	86	bottom	18.6 (< 0.0001)[c]	

[a]Values in brackets are *P* values of Chi-Square test. [b]Expected ratio of 1 if *nmt1 nmt2 nmt3* allele ovules were distributed randomly along the silique or if *nmt1 nmt2 nmt3* pollinated ovules randomly along the whole silique. [c]denotes significantly different frequency from the expected 50% frequency

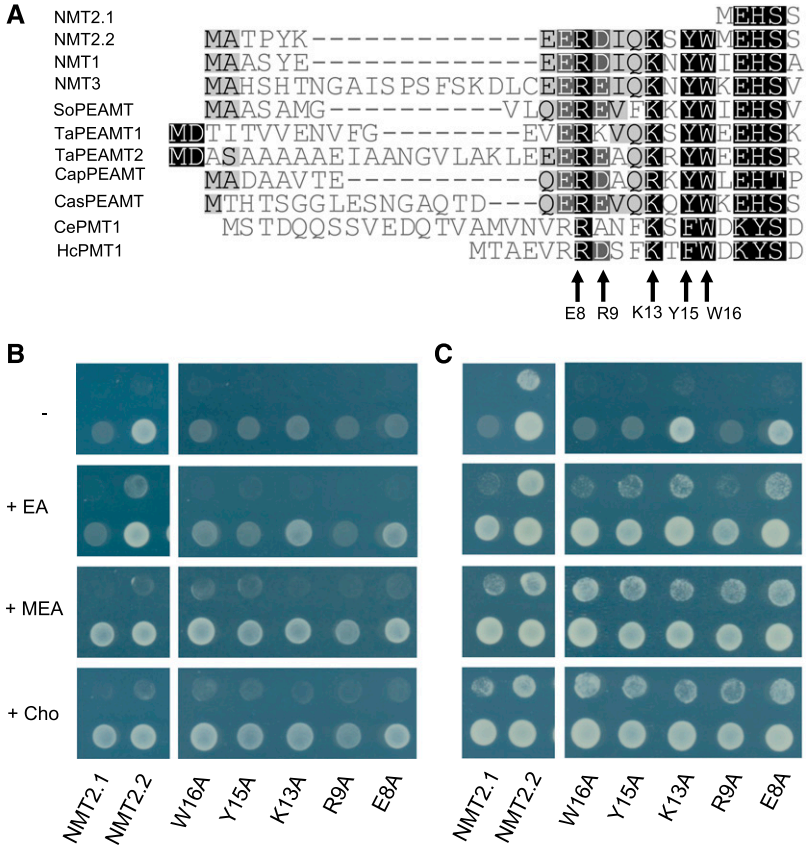

Figure 10. Five conserved residues at the N-terminal of NMT2.2 are critical for catalysis of PEA methylation. A, Alignment of the N-terminal sequences of NMT2.1 and biochemically verified PEAMTs from plants, algae, apicomplexans, and nematodes. Shown are NMT2.2 (Arabidopsis thaliana, NCBI, NM_202264.2), NMT1 (Arabidopsis thaliana, TAIR, At3g18000), NMT3 (Arabidopsis thaliana, TAIR, At1g73600), SoPEAMT (*Spinacia oleracea*, NCBI, Q9M571), TaPEAMT1 (*Triticum aestivum*, NCBI, AAL40895), TaPEAMT2 (*Triticum aestivum*, NCBI, ACV89824), CapPEAMT (*Chlamydomonas applanata*, NCBI, BAX38993), CasPEAMT (*Chlamydomonas asymmetrica*, NCBI, BAU37045), CePMT1 (*Caenorhabditis elegans*, NCBI, NP_494990), HcPMT1 (*Haemonchus contortus*, NCBI, AML60259). Used for alignment was ClustalW built in Geneious v7.1.3 (Biomatters) with default parameters. Identical and related amino acids that are conserved in 100%, 80%, and 60% of the sequences are highlighted in black, dark gray, and light gray, respectively. Conserved amino acids targeted for mutagenesis in (B) and (C) are indicated below the alignments. B and C, Yeast mutant strain *pem1*Δ *pem2*Δ transformed with pYES-DEST52 carrying *NMT2.1*, *NMT2.2*, or mutated *NMT2.2* variants NMT2.2W16A, NMT2.2Y15A, NMT2.2K13A, NMT2.2R9A, or NMT2.2E8A, were grown in minimal media supplemented with EA, MEA, or choline at 1 mM concentrations as indicated, and spotted after 2-d incubation (B) or 4 d (C), at two dilutions differing by a factor of 10 (1 and 0.1, bottom row and top row, respectively, within each subpanel).

pmt-2 at the L4 larva stage led to developmental arrest and lethality in the F1 progeny at the L1/L2 larval stage (for both knockdowns) or the L3 stage (for the *pmt-2* knockdown) (Palavalli et al., 2006; Brendza et al., 2007). Disruption of the unique *P. falciparum PEAMT/PMT* led to significant defects in parasite growth, multiplication, and viability but was not lethal (Witola et al., 2008). The authors attributed the survival of the mutated parasite to the presence of residual Cho in the human erythrocytes. The absolute need of PC for survival has also been observed in organisms where it is synthesized through the phosphatidyl-base methylation pathway. One example is provided by yeast mutant strains where the PC synthesis genes *CHO2/PEM1* and *OPI3/PEM2* are disrupted, causing PC deficiency and cell death (Kodaki and Yamashita, 1987; Preitschopf et al., 1993). Another example occurs in mice, where deletion of *PEMT* results in decreased PC concentrations in hepatic membranes, development of severe liver pathology, and death when fed a Cho deficient diet (Walkey et al., 1998; Waite et al., 2002). Thus, the requirement of PC synthesis for development and survival is evolutionarily conserved in eukaryotes.

Diversification of NMT Enzymatic Properties and Physiological Roles

Alternative promoter usage is one way to create gene expression divergence and/or proteins differing at the N terminus. About 50% of human coding genes possess more than one promoter (Kimura et al., 2006). Few plant studies have investigated alternative promoter

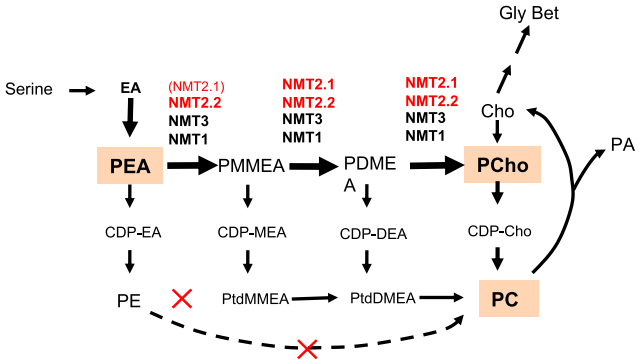

Figure 11. Revised model of de novo PC synthesis in Arabidopsis. Denoted in red are the findings of this study: a) The Arabidopsis P-base methylation pathway is catalyzed by four enzymes, three catalyzing all three methylation steps in planta—NMT1, NMT3, and NMT2.2—and a fourth PEAMT (NMT2.1) much less efficient in methylating PEA, hence mostly catalyzing the two subsequent methylations. b) PC cannot be produced directly from PE (red cross on curved dashed-arrow). c) The methylation of PEA to PMMEA is the sole entry point to PC synthesis (red cross denoting the absence of enzyme for the conversion of PE to PtdMMEA).

usage (Hernandez-Garcia and Finer, 2014). In this work we show that *NMT2* produces two transcripts through the use of alternative promoters. Analysis of the encoded proteins demonstrate that they are not biochemically and physiologically redundant in vivo, due to the combination of differences in expression patterns and catalytic properties (Figs. 1, 3, and 7), and likely also sensitivity to end-product concentrations (Fig. 8). NMT2.2 corresponds to the NMT2 protein recently characterized in in vitro enzymatic assays alongside NMT1 and NMT3 (Lee and Jez, 2017). Its high catalytic efficiency in converting PEA to PCho, observed in our ^{31}P-NMR assays, is similar to NMT1 (Fig. 1; Chen et al., 2018) and it is consistent with the kinetic parameters reported in that study. Our data show that NMT2.2 functions as a PEAMT in planta. This functionality is established by its ability to complement the *nmt1* short root phenotype and to maintain PC synthesis and growth in the *nmt1 nmt3* mutant.

The NMT2.1 isoform corresponds to the NMT2 variant reported by BeGora et al. (2010) as being unable to form PMMEA from PEA and thus as a PMEAMT enzyme catalyzing the next two methylations only. In our study, we found that NMT2.1 has limited capacity (but yet some) to methylate PEA, through two different approaches (Figs. 1 and 3). The discrepancy between our present study and BeGora et al. (2010)'s could lie in differences in experimental conditions. Another possible explanation is the longer time course of our assays, because the ability of NMT2.1 to convert PEA to PCho only became apparent after a significant lag phase. Regardless, the absence of detectable phenotypic complementation by *ProNMT1:NMT2.1* of the defects induced by PC deficiency in *nmt1* roots suggests a low contribution of NMT2.1 to the first phospho-base methylation of PEA in planta, under physiological EA levels. Further studies under a range of growth conditions are required to determine whether it is nil. However, our results leave little doubt that the production of PMMEA to sustain the formation of PC and plant life relies by and large on NMT1, NMT3, and NMT2.2 in the wild-type Arabidopsis.

All characterized plant PEAMT enzymes have a bipartite structure with two functional AdoMet-dependent catalytic domains, one at the N terminus (MT1 domain) catalyzing the first methylation of PEA to PMEA, the other (MT2) at the C terminus catalyzing the two subsequent methylations to produce PCho (Bolognese and McGraw, 2000; Nuccio et al., 2000; Charron et al., 2002; Lee and Jez, 2017). NMT2.1 and NMT2.2 have identical catalytic N- and C-domains, and only differ by 16 AAs, upstream of MT1. Our data provide biochemical, genetic, and physiological evidence for the importance of that initial AA stretch in determining the differential efficiency of the two isoforms in catalyzing the P-base pathway, in particular its first step. Specifically, five conserved AAs among those 16 are identified as playing major roles, with three of them being individually absolutely necessary for PEAMT activity (Fig. 10). Most interestingly, the recently released crystal structure of NMT2.2 shows that these 16 AAs form a β1e-α7 loop that encloses the MT1 active catalytic site following binding of substrates (Lee and Jez, 2017). Positioning the critical E8, R9, K13, Y15, and W16 residues on the published quaternary structure of the enzyme in complex (5WP5; http://wwwpdb.org/) suggests that these all-polar AA may be important for docking the substrates on the enzyme MT1 catalytic site (Supplemental Figure S7). Future studies are required to test that proposition and test the role of these critical AAs in the structural rearrangements and dynamic conformational changes that occur during the formation of a functional MT1 active site and catalysis of PEA methylation (Lee and Jez, 2017).

Together with our earlier study (Chen et al., 2018), the present work establishes that the vital phosphobase methylation pathway is catalyzed by a family of four nontotally redundant proteins in Arabidopsis—proteins with, furthermore, unequal contribution to the production of PC. The absence of an overt phenotype or detectable modifications of lipid profiles in *nmt2* or *nmt3* single mutants indicates that under optimal conditions, *NMT3, NMT2.2,* and *NMT2.1* are individually and collectively dispensable. In the absence of *NMT1*, however, *NMT3* becomes necessary to maintain normal development of leaves, roots, and reproductive organs and normal fertility; while loss of *NMT2* is more innocuous, only slowing down stem elongation (Fig. 5). However, when NMT1 and NMT3 are both lost, residual NMT2 function maintains pollen fitness and prevents complete embryo lethality and plant sterility (Fig. 9). A significant contribution of NMT2 to pollen tube growth is consistent with *NMT2* preferential expression in pollen, in its two forms (Fig. 7). A role in stem elongation is more intriguing. Even more interesting is that *NMT2* can alone rescue *nmt1 nmt3*

seedlings from death, and that *NMT2* can enable them to synthesize PC and to create compositionally modified, but still functional, cellular membranes throughout the plant. Indeed, expression of NMT2.2 appears to be mostly confined to the root cap and later, to flowers (Fig. 7). Yet, NMT2.2 is the only one of the two NMT2 gene products capable of efficiently catalyzing the formation of PMEA from PEA, i.e. the vital step committing to PC. Cho movement has been widely documented in mammals. In plants, Cho is found in the plant vasculature; and the rescue of the *nmt1 nmt2 nmt3* mutant by exogenous Cho supply (Fig. 5) also shows that Cho can be transported throughout the plant. Consistently, a Cho transporter homologous to the mammalian CTL Cho transporter-like has recently been identified in Arabidopsis, and implicated in the formation of plasmodesmata and phloem sieve-plate (Dettmer et al., 2014; Kraner et al., 2017). In the light of this finding and of the overlapping but also broader expression of *NMT2.1* (in particular in the whole vasculature), an appealing scenario would be where the two NMT2 variants "cooperate" NMT2.2 ensuring PMEA is formed, even if only very locally, NMT2.1 facilitating its fast removal via conversion to PCho and subsequent transport to neighbouring cells and distant tissues, thereby limiting the accumulation of MEA and maintaining NMT2.2 PEAMT activity as high as possible to sustain minimum PC synthesis and survival. It will be intriguing to probe that scenario in future research.

Gene duplication and divergence contribute to evolutionary novelty (Ohno, 1970) and morphological complexity (Freeling and Thomas, 2006). Duplicates can be retained via mutations leading to gain of a new function (neo-functionalization), division of ancestral functions among duplicates (subfunctionalization), and dosage selection (Conant and Wolfe, 2008; Panchy et al., 2016). *AtNMT1* and *AtNMT2* map to duplicated segments of chromosomes 3 and 1, respectively, indicating that they originate from a recent gene duplication event (The Arabidopsis Genome Initiative, 2000; Lee et al., 2013). The conserved function and similar catalytic properties of NMT1 and NMT2.2 (herein and Lee and Jez, 2017) suggest that *NMT2.2* likely corresponds to the original duplicate, while *NMT2.1* evolved through mutations in the promoter and 5′ end regions, which led to: modified expression patterns (Fig. 7); loss of the uORF (Fig. 2); decreased sensitivity to end-product feedback inhibition (Fig. 8; Tabuchi et al., 2006; Alatorre-Cobos et al., 2012); and loss of key N-terminal residues necessary for efficient methylation of PEA (Fig. 10). One may then wonder why such a protein variant with limited capacity to accept PEA as a substrate, i.e. to catalyze the vital committing step of the P-base methylation pathway, would be desirable. Being sessile, plants are unavoidably exposed to large and dynamic variations in their environment. Plants confront a range of abiotic stresses, prominently drought and osmotic stress, to which they commonly adapt through down-regulation of cellular proliferation or even temporary growth arrest. This adaptation requirement implies the need for fine-tuned mechanisms allowing for down-regulation of sink activity and building cellular protection. An enzyme like NMT2.1 that is broadly expressed, at levels similar to NMT1 (Supplemental Figure S6), and has high affinity for PMEA and PDMEA (Lee and Jez, 2017) but lower susceptibility to PCho feedback inhibition (Fig. 8), may help channel PMMEA to PCho synthesis anddownstream Gly betaine synthesis. This would help promote osmoregulation and the widespread roles Gly betaine appears to have in stress tolerance (Park et al., 2007; Chen and Murata, 2008, 2011). NMT2.1 may also help channel PMMEA to the production of signaling molecules and TAG storage lipids (Supplemental Figure S3C; Chen et al., 2018), rather than to membrane synthesis.

In summary, we demonstrate the absolute necessity of phosphoethanolamine methyltransferase activity for de novo PC synthesis and plant survival, and identify key conserved residues conditioning catalysis of the vital commitment step of the Ser-derived phospho-base methylation pathway. This opens fresh avenues for enzymatic engineering and the exploration of ways to better tune PC synthesis and lipid metabolism to environmental conditions for improved plant performance.

MATERIALS AND METHODS

Plant Materials and Growth Conditions

Arabidopsis ecotype Col-0 was used as the wild type. Knock-out T-DNA mutants *nmt1* and *nmt3*, (SALK_036291) and (SAIL_22_D10), respectively, and we isolated the double *nmt1 nmt3* mutant as described (Chen et al., 2018). T-DNA insertion lines *nmt2* (SALK_204065C) and (SALK_006037) were obtained from ABRC (http://www.arabidopsis.org/abrc/). Homozygous plants were isolated through PCR genotyping, using primers 306, 1987, and 2552 (*nmt2* line), and primers 1770, 1771, and 464 (SALK_006037 line). The homozygous *nmt1 nmt2 nmt3* triple mutant was created through the crossing of *nmt1 nmt2* and *nmt2 nmt3* double mutants, and PCR genotyping of the F2 progeny grown on media supplemented with Cho was conducted using the above primers for *nmt2,* and primers 1988, 1989, and 1987 (*nmt1*), and 451, 452, and 455 (*nmt3*). Primer sequences are listed in Supplemental Table S1.

Plants were grown as previously described (Chen et al., 2018), unless otherwise specified, on solid media or soil.

Transgenic Plants

The coding sequence of *NMT2.1* and *NMT2.2* were amplified by PCR using primer pairs 2396/2175 and 2176/2175, respectively (Supplemental Table S1). The resultant PCR products were introduced into pDONR207 through BP reaction according to the manufacturer's instructions (Thermo-Fisher Scientific), resulting in pDONR207:NMT2.1 and pDONR207:NMT2.2, respectively. The *NMT1* promoter was amplified by PCR using primer pair 1898/1794 (Supplemental Table S1). The PCR product was cloned into pDONRP4P1r through BP reaction resulting in pDONRp4p1r:NMT1Pro3. To facilitate the screen of transgenic seeds, we introduced the DNA fragment containing the fluorescence marker OLE1-RFP under the control of pOLE1 flanked by *Hind*III sites from pFASTR06 (Shimada et al., 2010) into pH7m24GW.3, producing pWHC242. Promoter gene fusions NMT1Pro3:NMT2.1 and NMT1Pro3: NMT2.2 were generated by recombining pDONR207:NMT2.1 and pDONR207: NMT2.2, respectively, with pDONRp4p1r:NMT1Pro3 into the destination vector pWHC242.

The genomic sequence of *NMT2* including UTRs was amplified by PCR using primer pair 1764/1765, and cloned into pDONR207 through BP reaction, yielding the pDONR207:NMT2gDNA vector. The *NMT1Pro1:gNMT2*

fusion was generated by a recombination of pDONR207:NMT2gDNA with pDONRP4P1r:NMT1Pro1 (Chen et al., 2018) into the multisite destination vector pWHC100, yielding the destination vector pWHC100:NMT1Pro1:NMT2gDNA. The *NMT1Pro* (including the uORF) used to drive NMT2 expression was amplified by PCR using primer pair 1793/1794. For generating the *ProNMT2.1:GUS* and *ProNMT2.2:GUS* promoter fusion, *NMT2.1* and *NMT2.2* promoter fragments were amplified by PCR using Col-0 genomic DNA as a template with primer pairs 2444/2469 and 2444/2443, respectively. For creating the delta promoter *GUS* fusion (*DeltaPro:GUS*), a DNA fragment was amplified from Col-0 genomic DNA with primer pair 2686/2469. The resulting PCR products were introduced into pDONR207 and subsequently recombined into the pFASTG04 (Shimada et al., 2010) destination vector using Gateway cloning technology (Thermo-Fisher Scientific). The expression vectors were transformed into *Agrobacterium tumefaciens* strain *Gv3101* by electroporation. The *A. tumefaciens*-mediated floral dip method (Davis et al., 2009) was used for Arabidopsis transformation. *NMT1Pro3:NMT2.1, NMT1Pro3:NMT2.2,* and *NMT1Pro1:NMT2gDNA* were transformed into *nmt1* mutant background, and *ProNMT2.1:GUS* and *ProNMT2.2:GUS* and *DeltaPro:GUS* were transformed into the WT background. All PCR reactions for cloning were carried out using Phusion DNA Polymerase (Finnzymes) according to the manufacturer's instructions.

^{13}C-ethanolamine Labeling and Liquid Chromatography-Mass Spectrometry (LC-MS) Lipid Analysis

Seven-day-old Arabidopsis seedlings grown on 1/2 MS medium with 1% Suc, 1.2% agar were transferred into liquid media (1/2 MS with 1% Suc, pH 5.8) with 250-μM ^{13}C-ethanolamine for up to 8 h, followed by shaking at 150 rpm and incubation at 21°C with a light intensity of 120-μmol m^{-2} s^{-1}. Samples were rinsed with water and snap-frozen in liquid nitrogen at time t_0 (beginning of incubation) and after 30 min, 1 h, 2 h, 4 h, and 8 h incubation.

Lipid extraction from freeze-dried tissues, and lipid profiling were performed as previously described (Chen et al., 2018). Cho and PCho were analyzed by liquid chromatography-tandem mass spectrometry (LC-MS/MS) in freeze-dried tissues. All solvents were LC-MS grade and purchased from Biosolve (Valkenswaard, The Netherlands). Standard compounds were obtained from Sigma Aldrich (Saint-Quentin Fallavier, France). A pool of reference standard solutions was prepared and serially diluted in water to obtain 7 standard solutions ranging from 0.1 to 100 μmol/L. Standard solutions were then dried under a nitrogen stream (45°C), and freeze-dried tissues (20 mg) were mechanically homogenized. Standard and tissue samples were dissolved in 600 μL of a methanol:chloroform:water mixture (6:2:2, v/v/v) containing $^{2}H_9$-choline (50 μmol/L) as labeled internal standard. Biological samples were incubated on ice for 10 min and mixed with 450 μL of water and 50 μL of chloroform for phase enlargement. After centrifugation (1 min, 14,000*g*), the upper phase was dried under a nitrogen stream for 45 min (45°C). Dried samples were finally solubilized in 50 μL of acetonitrile and then injected into the LC-MS/MS system. Analyses were performed on a Xevo TQD mass spectrometer with an electrospray interface and an Acquity H-Class UPLC device (Waters Corporation, Milford, MA, USA). Samples (10 μL) were injected onto a HILIC-BEH column (1.7 μm; 2.1 × 100 mm, Waters Corporation) held at 30°C, and compounds were separated with a linear gradient of mobile phase B (98% v/v acetonitrile, 0.1% v/v formic acid) in mobile phase A (10-mmol/L ammonium acetate, 0.1% v/v formic acid) at a flow rate of 400 μL/min. Mobile phase A was kept constant for 1 min at 1%, linearly increased from 1% to 45% for 6.5 min, kept constant for 0.5 min, returned to the initial condition over 1.5 min, and kept constant for 2.5 min before the next injection. Targeted compounds were then detected by the mass spectrometer with the electrospray interface operating in the positive ion mode (capillary voltage, 1.5 kV; desolvatation gas (N_2) flow and temperature, 650 L/h and 350°C; source temperature, 150°C). The multiple reaction monitoring mode was applied for MS/MS detection with the following mass-to-charge (*m/z*) transitions: choline, *m/z* 104.1 → 60.1 (cone and collision voltage set at 40 and 15 V, respectively), $^{2}H_9$-choline, *m/z* 113.2 → 69.1 (cone and collision voltage set at 40 and 15 V, respectively), and phosphocholine, *m/z* 184.0 → 86.0 (cone and collision voltage set at 35 and 20 V, respectively). Chromatographic peak area ratios between targeted compounds and their internal standard constituted the detector responses. Standard solutions were used to plot calibration curves for quantification and dilution factors related to biological matrix preparations were included in the calculation. The linearity was expressed by the mean r^2, which was greater than 0.998 for both compounds (linear regression, 1/x weighting, origin excluded).

Transgenic Yeasts

The coding regions of *NMT2.1* and *NMT2.2* without the stop codon were amplified from Col-0 cDNA by PCR using primer pairs 2396/2192 and 2176/2192, respectively, and cloned into pDONR207 using Gateway technology (Thermo-Fisher Scientific), resulting in pDONR207:NMT2.1-TAA and pDONR207:NMT2.2-TAA. These clones were transferred into the pYES-DEST52 vector (Thermo-Fisher Scientific), resulting in pYES-DEST52:NMT2.1-TAA and pYES-DEST52:NMT2.2-TAA, respectively. These vectors as well as the pYES-DEST52:NMT1 vector (Chen et al., 2018) and empty vector pYES-DEST52 were transformed into *Saccharomyces cerevisiae pem1*Δ *pem2*Δ (MATα hisΔ3I leu2Δ0 ura3Δ0 pem1::Kanr -pem2::Kanr) (Pessi et al., 2005).

Site-directed mutagenesis was performed on the pDONR207:NMT2.2-TAA using PCR with primers containing the desired changes (2459/2458 [E8A], 2457/2456 [R9A], 2455/2454 [K13A], 2453/2452 [Y15A], 2451/2450 [W16A]) (Supplemental Table S1). Following the PCR reaction, the product was digested with DpnI and subsequently transformed into *E. coli* strain DH10B competent cells. Mutations were confirmed by sequencing and subsequently subcloned into pYES-DEST52. These expression vectors were transformed into *S. cerevisiae pem1*Δ *pem2*Δ (Pessi et al., 2005).

For spotting assays, transformed yeast single colonies were grown on liquid YNB media with 2% (w/v) Glc, 1-mM choline and amino acids His (20 μg/ml), Leu (30 mg/ml), and Met (20 μg/ml) at 28°C, with 200-rpm agitation until the OD_{600} reached about 1. Cells were harvested by centrifugation at 10,000g for 5 min followed by three washes. After normalization of OD_{600}, 10-μl of yeast cells were spotted on solid YNB media with amino acids as above and 2% Glc or 2% Gal, as indicated. 1-mM Cho was supplied as indicated. Plates were incubated at 37°C for two to four days.

For ^{31}P-NMR assays, *S. cerevisiae pem1*Δ *pem2*Δ cells harboring *pYESDEST52*, *pYES-DEST52:NMT1*, *pYESDEST52:NMT2.1*, or *pYESDEST52:NMT2.2* were grown in liquid YNB media with 2% Gal, 1-mM Cho, and amino acids His (20 μg/ml), Leu (30 mg/ml), and Met (20 μg/ml) at 28°C, 200-rpm agitation. Crude protein extracts were obtained as previously described (Chen et al., 2018). ^{31}P-NMR was used to monitor the formation of PCho from PEA in extracts of equal protein concentrations, following initiation of the reaction by adding 5-mM PEA and 15-mM S-Adenosyl Met substrates, and 5-mM methylphosphonate as an internal standard (Rueppel and Marvel, 1976), to the desalted proteins in a final volume of 400 μl in HED buffer (time zero). ^{31}P-NMR spectra were recorded as previously described (Chen et al., 2018) over a time course of 4 to 5 d.

Reverse Transcription Quantitative PCR Analysis

RNA isolation, reverse transcription, and quantitative PCR were carried out as previously described (Chen et al., 2018) on a minimum of four biological replicates per sample. Primers used are listed in Supplemental Table S2. Results are expressed as fold change in expression normalized to the geometric mean of three reference genes: *APT1*, *PDF2*, and *GAPDH*.

Accession Numbers

Sequence data from this article can be found in the Arabidopsis Genome Initiative or GenBank/EMBL databases under accession numbers: *NMT1* (At3g18000), *NMT3* (At1g73600), *NMT2* (At1g48600), *NMT2.1* (NM_103756.3), *NMT2.2* (NM_202264.2), *APT1* (At1g27450), *PDF2/PP2AA3* (At1g13320), and *GAPDH* (AT1G13440).

Supplemental Data

The following supplementary material is available:

Supplemental Figure S1. Routes of PC synthesis in plants, yeast, and mammals.

Supplemental Figure S2. Molecular characterization of T-DNA SALK_204065C and SALK_006037 insertional mutants.

Supplemental Figure S3. Concentrations of major lipids in the wild type and *nmt1*, *nmt2*, *nmt3*, *nmt1 nmt2*, *nmt2 nmt3*, *nmt1 nmt3*, and *nmt1 nmt2 nmt3* knock-out mutants.

Supplemental Figure S4. Molecular species of major lipids in the wild type and all combinations of *nmt* mutants.

Supplemental Figure S5. Exogenous choline supply restores the wild type development in the otherwise lethal *nmt1 nmt2 nmt3* triple mutant.

Supplemental Figure S6. *NMT2.1* and *NMT2.2* expression levels compared to *NMT1* and *NMT3,* and the promoter region controlling differences in their spatial expression.

Supplemental Figure S7. Positions of five conserved critical amino acids on the NMT2.2 crystal structure.

Supplemental Table S1. List of genotyping and cloning primers.

Supplemental Table S2. List of primers used for semiquantitative and quantitative PCR.

ACKNOWLEDGMENTS

We thank the ABRC for the supply of *nmt* seeds. We appreciate the support of the Australian National University (ANU) and the Grains Research and Development Corporation.

Received June 8, 2018; accepted October 19, 2018; published October 31, 2018.

LITERATURE CITED

Alatorre-Cobos F, Cruz-Ramírez A, Hayden CA, Pérez-Torres C-A, Chauvin A-L, Ibarra-Laclette E, Alva-Cortés E, Jorgensen RA, Herrera-Estrella L (2012) Translational regulation of Arabidopsis XIPOTL1 is modulated by phosphocholine levels via the phylogenetically conserved upstream open reading frame 30. J Exp Bot **63:** 5203–5221

Baud S, Dubreucq B, Miquel M, Rochat C, Lepiniec L (2008) Storage Reserve Accumulation in Arabidopsis: Metabolic and Developmental Control of Seed Filling. Arabidopsis Book **6:** e0113

BeGora MD, Macleod MJR, McCarry BE, Summers PS, Weretilnyk EA (2010) Identification of phosphomethylethanolamine *N*-methyltransferase from arabidopsis and its role in choline and phospholipid metabolism. J Biol Chem **285:** 29147–29155

Bolognese CP, McGraw P (2000) The isolation and characterization in yeast of a gene for arabidopsis s-adenosylmethionine:Phospho-ethanolaminen-methyltransferase. Plant Physiol **124:** 1800–1813

Bremer J, Greenberg DM (1961) Methyl transfering enzyme system of microsomes in the biosynthesis of lecithin (phosphatidylcholine). Biochim Biophys Acta **46:** 205–216

Brendza KM, Haakenson W, Cahoon RE, Hicks LM, Palavalli LH, Chiapelli BJ, McLaird M, McCarter JP, Williams DJ, Hresko MC, Jez JM (2007) Phosphoethanolamine *N*-methyltransferase (pmt-1) catalyses the first reaction of a new pathway for phosphocholine biosynthesis in *Caenorhabditis elegans.* Biochem J **404:** 439–448

Charron J-BF, Breton G, Danyluk J, Muzac I, Ibrahim RK, Sarhan F (2002) Molecular and biochemical characterization of a cold-regulated phosphoethanolamine *N*-methyltransferase from wheat. Plant Physiol **129:** 363–373

Chen TH, Murata N (2008) Glycinebetaine: An effective protectant against abiotic stress in plants. Trends Plant Sci **13:** 499–505

Chen TH, Murata N (2011) Glycinebetaine protects plants against abiotic stress: Mechanisms and biotechnological applications. Plant Cell Environ **34:** 1–20

Chen W, Salari H, Taylor MC, Jost R, Berkowitz O, Barrow R, Qiu D, Branco R, Masle J (2018) NMT1 and NMT3 *N*-methyltransferase activity is critical to lipid homeostasis, morphogenesis and reproduction in Arabidopsis. Plant Physiol

Conant GC, Wolfe KH (2008) Turning a hobby into a job: How duplicated genes find new functions. Nat Rev Genet **9:** 938–950

Cruz-Ramírez A, López-Bucio J, Ramírez-Pimentel G, Zurita-Silva A, Sánchez-Calderon L, Ramírez-Chávez E, González-Ortega E, Herrera-Estrella L (2004) The *xipotl* mutant of Arabidopsis reveals a critical role for phospholipid metabolism in root system development and epidermal cell integrity. Plant Cell **16:** 2020–2034

Cui Z, Vance JE, Chen MH, Voelker DR, Vance DE (1993) Cloning and expression of a novel phosphatidylethanolamine *N*-methyltransferase: A specific biochemical and cytological marker for a unique membrane fraction in rat liver. J Biol Chem **268:** 16655–16663

Datko AH, Mudd SH (1988a) Phosphatidylcholine synthesis: Differing patterns in soybean and carrot. Plant Physiol **88:** 854–861

Datko AH, Mudd SH (1988b) Enzymes of phosphatidylcholine synthesis in *Lemna,* soybean, and carrot. Plant Physiol **88:** 1338–1348

Davis AM, Hall A, Millar AJ, Darrah C, Davis SJ (2009) Protocol: Streamlined sub-protocols for floral-dip transformation and selection of transformants in Arabidopsis thaliana. Plant Methods **5:** 1–7

Dettmer J, Ursache R, Campilho A, Miyashima S, Belevich I, O'Regan S, Mullendore DL, Yadav SR, Lanz C, Beverina L, Papagni A, Schneeberger K, et al (2014) CHOLINE TRANSPORTER-LIKE1 is required for sieve plate development to mediate long-distance cell-to-cell communication. Nat Commun **5:** 1–11

Freeling M, Thomas BC (2006) Gene-balanced duplications, like tetraploidy, provide predictable drive to increase morphological complexity. Genome Res **16:** 805–814

Hayden CA, Jorgensen RA (2007) Identification of novel conserved peptide uORF homology groups in Arabidopsis and rice reveals ancient eukaryotic origin of select groups and preferential association with transcription factor-encoding genes. BMC Biol **5:** 32

Hernandez-Garcia CM, Finer JJ (2014) Identification and validation of promoters and cis-acting regulatory elements. Plant Sci **217:** 109–119

Hitz WD, Rhodes D, Hanson AD (1981) Radiotracer evidence implicating phosphoryl and phosphatidyl bases as intermediates in betaine synthesis by water-stressed barley leaves. Plant Physiol **68:** 814–822

Kennedy EP, Weiss SB (1956) The function of cytidine coenzymes in the biosynthesis of phospholipides. J Biol Chem **222:** 193–214

Keogh MR, Courtney PD, Kinney AJ, Dewey RE (2009) Functional characterization of phospholipid *N*-methyltransferases from Arabidopsis and soybean. J Biol Chem **284:** 15439–15447

Kimura K, Wakamatsu A, Suzuki Y, Ota T, Nishikawa T, Yamashita R, Yamamoto J, Sekine M, Tsuritani K, Wakaguri H, Ishii S, Sugiyama T, et al (2006) Diversification of transcriptional modulation: Large-scale identification and characterization of putative alternative promoters of human genes. Genome Res **16:** 55–65

Kodaki T, Yamashita S (1987) Yeast phosphatidylethanolamine methylation pathway: Cloning and characterization of two distinct methyltransferase genes. J Biol Chem **262:** 15428–15435

Kraner ME, Link K, Melzer M, Ekici AB, Uebe S, Tarazona P, Feussner I, Hofmann J, Sonnewald U (2017) Choline transporter-like1 (CHER1) is crucial for plasmodesmata maturation in Arabidopsis thaliana. Plant J **89:** 394–406

Lee SG, Jez JM (2017) Conformational changes in the di-domain structure of Arabidopsis phosphoethanolamine methyltransferase leads to active site formation. J Biol Chem **292:** 21690–21702

Lee TH, Tang H, Wang X, Paterson AH (2013) Pgdd: A database of gene and genome duplication in plants. Nucleic Acids Res **41:** D1152–D1158

Liu Y, Wang G, Wang X (2015) Role of amino alcohol phosphotransferases 1 and 2 in phospholipid homeostasis in Arabidopsis. Plant Cell **27:** 1512–1528

McGraw P, Henry SA (1989) Mutations in the *saccharomyces cerevisiae* opi3 gene: Effects on phospholipid methylation, growth and cross-pathway regulation of inositol synthesis. Genetics **122:** 317–330

McNeil SD, Nuccio ML, Rhodes D, Shachar-Hill Y, Hanson AD (2000) Radiotracer and computer modeling evidence that phospho-base methylation is the main route of choline synthesis in tobacco. Plant Physiol **123:** 371–380

Mou Z, Wang X, Fu Z, Dai Y, Han C, Ouyang J, Bao F, Hu Y, Li J (2002) Silencing of phosphoethanolamine *N*-methyltransferase results in temperature-sensitive male sterility and salt hypersensitivity in Arabidopsis. Plant Cell **14:** 2031–2043

Mudd SH, Datko AH (1986) Phosphoethanolamine bases as intermediates in phosphatidylcholine synthesis by *Lemna*. Plant Physiol **82:** 126–135

Nuccio ML, Ziemak MJ, Henry SA, Weretilnyk EA, Hanson AD (2000) cDNA cloning of phosphoethanolamine *N*-methyltransferase from spinach by complementation in *Schizosaccharomyces pombe* and characterization of the recombinant enzyme. J Biol Chem **275:** 14095–14101

Ohno S (1970) Evolution by gene duplication. Springer-Verlag, Berlin

Palavalli LH, Brendza KM, Haakenson W, Cahoon RE, McLaird M, Hicks LM, McCarter JP, Williams DJ, Hresko MC, Jez JM (2006) Defining the role of phosphomethylethanolamine *N*-methyltransferase from caenorhabditis elegans in phosphocholine biosynthesis by biochemical and kinetic analysis. Biochemistry **45:** 6056–6065

Panchy N, Lehti-Shiu M, Shiu S-H (2016) Evolution of gene duplication in plants. Plant Physiol **171:** 2294–2316

Park EJ, Jeknic Z, Pino MT, Murata N, Chen TH (2007) Glycinebetaine accumulation is more effective in chloroplasts than in the cytosol for protecting transgenic tomato plants against abiotic stress. Plant Cell Environ **30:** 994–1005

Pessi G, Kociubinski G, Mamoun CB (2004) A pathway for phosphatidylcholine biosynthesis in *plasmodium falciparum* involving phosphoethanolamine methylation. Proc Natl Acad Sci USA **101:** 6206–6211

Pessi G, Choi J-Y, Reynolds JM, Voelker DR, Mamoun CB (2005) In vivo evidence for the specificity of *plasmodium falciparum* phosphoethanolamine methyltransferase and its coupling to the Kennedy pathway. J Biol Chem **280:** 12461–12466

Preitschopf W, Lückl H, Summers E, Henry SA, Paltauf F, Kohlwein SD (1993) Molecular cloning of the yeast opi3 gene as a high copy number suppressor of the cho2 mutation. Curr Genet **23:** 95–101

Rueppel ML, Marvel JT (1976) 1H and 31P NMR spectra of substituted methylphosphonic acids with indirect determination of 31P shifts. Org Magn Reson **8:** 19–20

Shimada TL, Shimada T, Hara-Nishimura I (2010) A rapid and non-destructive screenable marker, fast, for identifying transformed seeds of Arabidopsis thaliana. Plant J **61:** 519–528

Summers PS, Weretilnyk EA (1993) Choline synthesis in spinach in relation to salt stress. Plant Physiol **103:** 1269–1276

Summers EF, Letts VA, McGraw P, Henry SA (1988) *Saccharomyces cerevisiae* cho2 mutants are deficient in phospholipid methylation and cross-pathway regulation of inositol synthesis. Genetics **120:** 909–922

Tabuchi T, Okada T, Azuma T, Nanmori T, Yasuda T (2006) Post-transcriptional regulation by the upstream open reading frame of the phosphoethanolamine *N*-methyltransferase gene. Biosci Biotechnol Biochem **70:** 2330–2334

The Arabidopsis Genome Initiative (2000) Analysis of the genome sequence of the flowering plant Arabidopsis thaliana. Nature **408:** 796–815

Waite KA, Cabilio NR, Vance DE (2002) Choline deficiency–induced liver damage is reversible in pemt−/− mice. J Nutr **132:** 68–71

Walkey CJ, Yu L, Agellon LB, Vance DE (1998) Biochemical and evolutionary significance of phospholipid methylation. J Biol Chem **273:** 27043–27046

Welti R, Li W, Li M, Sang Y, Biesiada H, Zhou H-E, Rajasekar B, Williams TD, Wang X (2002) Profiling membrane lipids in plant stress responses: Role of phospholipase Dα in freezing-induced lipid changes in Arabidopsis. J Biol Chem **277:** 31994–32002

Witola WH, El Bissati K, Pessi G, Xie C, Roepe PD, Mamoun CB (2008) Disruption of the *plasmodium falciparum PfPMT* gene results in a complete loss of phosphatidylcholine biosynthesis via the serine-decarboxylase-phosphoethanolamine-methyltransferase pathway and severe growth and survival defects. J Biol Chem **283:** 27636–27643

Yeagle PL (2016) PL Yeagle, ed, The Membranes of Cells., 3rd. Academic Press, Amsterdam, pp 291–334